Biomass and Bioenergy 204 (2026) 108456

Contents lists available at ScienceDirect

Biomass and Bioenergy

journal homepage: www.elsevier.com/locate/biombioe

Two-step hydrothermal liquefaction of waste biomass for increased bio-oil yield and enhanced bio-oil composition

Christyfani Sindhuwati [a,b], Mohamad A. Nahil [a], Paul T. Williams [a,*]

[a] School of Chemical and Process Engineering, University of Leeds, Leeds, LS2 9JT, UK
[b] Chemical Engineering Department, Politeknik Negeri Malang, Malang, Indonesia

ARTICLE INFO

Keywords:
Hydrothermal liquefaction
Biomass
Supercritical water: bio-oil

ABSTRACT

The process of hydrothermal liquefaction of waste biomass was executed through a subcritical water reaction, subsequently followed by a supercritical water reaction, with the objective of improving both the yield of bio-oil and the quality of its composition. The bio-oil, aqueous phase, and gas compositions were meticulously analysed to provide an in-depth understanding of how the separation of subcritical and supercritical process conditions affects the yield and composition of the products. The findings indicated that the two-step process yielded a greater amount of bio-oil in comparison to the direct supercritical water processing of the biomass. The highest yield of bio-oil achieved through the two-step process was 25.44 wt%, realised with a biomass to water ratio of 1:10. This involved an initial subcritical water reaction at a temperature of 250 °C for 30 min, succeeded by a second stage at a supercritical water temperature of 400 °C for a duration of 60 min. The bio-oil generated through the two-step process exhibited a greater proportion of longer-chain hydrocarbons, alongside elevated concentrations of phenolic compounds, oxygenated substances, terpenoids, and furans. Furthermore, there was a notable decrease in both the concentration and complexity of nitrogen-containing compounds. The gas composition generated in the two-step process primarily consisted of carbon dioxide, methane, carbon monoxide, and hydrogen, with an enhanced yield observed in this method when compared to direct supercritical water liquefaction. The examination of the residual aqueous phase revealed that acetic acid was the predominant compound, succeeded by formic acid, furfural, guaiacol, furan, phenol, and cresols, with these substances being generated in greater concentrations through the two-step process.

1. Introduction

Among other renewable energy sources, the use of biomass as a sustainable biofuel feedstock represents a promising alternative to fossil fuels. Liquid biofuels are functionally comparable to fossil fuels, and bio-oils generated from biomass have been thoroughly investigated recently as viable replacements to fossil fuels due to their renewable origin and compatibility with existing infrastructures [1]. The hydrothermal liquefaction of biomass for bio-oil production has become a viable method for converting biomass into liquid biofuel. Bio-oil is a liquid biofuel generated through the liquefaction of biomass via high-temperature, high-pressure thermal processing in the liquid phase.

Bio-oil comprises a complex mixture of oxygenated organic compounds with a broad molecular weight range, serving as a direct substitute for fuel oil in various applications, including boilers, furnaces, engines, and turbines for heat and power generation. It may also serve as intermediates for the synthesis of advanced fuels or chemicals through upgrading [2–4]. Bio-oils serve as abundant sources of various bio-based chemicals and products, including adhesive resins and asphalt substitutes [5,6]. Lignocellulose biomass is acknowledged as a highly promising feedstock to produce biofuels and bio-based chemicals, attributed to its wide availability and environmental sustainability [7].

The hydrothermal liquefaction process employs water as the reaction solvent, typically conducted at temperatures ranging from 260 to 350 °C and pressures between 5 and 21 MPa, with or without catalysts, to transform carbohydrates, proteins, lipids, and other macromolecular organic compounds in biomass into biofuel. Under hydrothermal liquefaction conditions, the diminished hydrogen bonds and reduced dielectric constant of water facilitate the decomposition of organic matter in the biomass feedstock [8,9]. Hydrothermal liquefaction transforms the majority of biomass into bio-oil in the presence of water. A significant drawback, however, is its incapacity to extract high

* Corresponding author.
E-mail address: p.t.williams@leeds.ac.uk (P.T. Williams).

https://doi.org/10.1016/j.biombioe.2025.108456
Received 19 August 2025; Received in revised form 30 September 2025; Accepted 1 October 2025
Available online 7 October 2025

value-added by-products or reclaim nutrients. Recent studies on sequential hydrothermal liquefaction aim to address this constraint by enabling the simultaneous extraction of co-products and improving bio-oil output. Sequential hydrothermal liquefaction comprises an initial subcritical phase characterised by prolonged residence time, succeeded by a subsequent supercritical water phase. The procedure offers essential advantages, including flexibility and agility.

By optimizing process conditions, reactions can be tailored to promote specific pathways and selectively recover various types of molecules. Furthermore, at an industrial scale, fractionation procedures must be customised to effectively separate and recover the intended products based on their inherent nature, characteristics, and specified properties, considering the multitude and diversity of product fractions and their unique attributes [10,11].

Sequential hydrothermal liquefaction fundamentally involves the extraction and transformation of biomass constituents, characterised by relatively high polarities and low thermal stabilities, such as sugars and proteins in the initial phase, followed by the less polar and more stable compounds, including lipids and lignin, in the subsequent phase [7,12]. Jazrawi et al. [13] observed that two-stage hydrothermal liquefaction of biomass yielded a bio-oil with 55 % lower nitrogen concentration compared to direct hydrothermal liquefaction. In a separate work, Ma et al. [14] examined microwave-assisted two-stage hydrothermal liquefaction of algae, revealing an elevated concentration of ketones in the resultant bio-oils. Motayaf et al. [15] employed a two-stage hydrothermal process, initiating with a first stage at 200 °C for 30 min, followed by a second stage at 300 °C for 30 min, resulting in the maximum nitrogen recovery in the aqueous phase and over 50 % energy recovery for bio-oil. Tong et al. [16] utilised sewage sludge as the biomass feedstock and conducted a two-stage hydrothermal treatment at 260 °C for 40 min in the first stage and 340 °C for 40 min in the second stage, achieving a maximum yield of bio-oil while demonstrating nitrogen migration and the formation of nitrogen-heterocycles and amides in the bio-oils. Wu et al. [17] examined the characteristics of biochar and the composition of bio-oil resulting from a two-stage hydrothermal treatment of dairy manure. Their research concentrated on generating value-added biochar, achieving a maximum nitrogen removal of 48 % during the initial stage at 200 °C for 1 h, followed by a second stage at 240−320 °C for 0.5−4 h, which resulted in an energy recovery of 44–68 % in the biochar. They also highlighted decarboxylation and dehydration mechanisms involved in the two-stage process along with reduced N content in the resulting bio-oils. In another study on animal manure, Long et al., [18], showed how two-stage hydrothermal treatment of swine manure resulted in enhanced bio-oil yields and quality, and they have emphasized detailed mechanisms on N migration and distribution for producing low-N bio-oils.

Several of the studies described above observed improved bio-oil yields and compositional quality using sequential hydrothermal liquefaction, however, while reporting promising results, these studies did not optimize performance. This work reports on the two-step subcritical-supercritical water liquefaction of biomass compared with the one-step supercritical water liquefaction of biomass. The yield and composition of the product bio-oil, aqueous phase and gases was determined and comparison made between the two processes to identify the key operating parameters, including temperature and reaction time. The aim of the work was to optimize process conditions to maximize the yield of bio-oil and also to determine the influence of such process conditions on the hydrocarbon composition of the bio-oil.

2. Materials and methods

2.1. Biomass

The biomass utilised in the study consisted of waste wood biomass sawdust pellets sourced from Liverpool Wood Pellets Ltd, Liverpool, UK. The biomass was comminuted and sieved to attain a particle size of 0.5–1 mm. The proximate and ultimate analyses (C, H, O, N, S) of wood, newspaper, cardboard, and polystyrene were conducted using a Schimadzu TGA-50 thermogravimetric analyser (TGA) and a Thermos EA-2000 elemental analyser, respectively. The proximate analysis results for the biomass showed a moisture content of 6.5 wt%, volatiles 78.4 wt %, fixed carbon 12.4 wt% and ash content of 2.6 wt%. The ultimate analysis results showed a carbon content of 50.2 wt%, hydrogen 6.5 wt %, oxygen content 43.0 wt% and nitrogen content of 0.3 wt%.

2.2. Hydrothermal liquefaction reactor

The hydrothermal liquefaction reactor was supplied by the Parr Instrument Company Inc. Illinois, USA, and was a Parr 4740 high-pressure vessel system with a volume capacity of 75 ml and constructed of T316 Stainless Steel. The reactor was heated with an external electric tube furnace provided by Elite Thermal System Limited. The reactor was equipped with a thermowell containing a thermocouple to detect its internal temperature, which was continuously monitored during the tests. The pressure within the reactor was generated by heating the water to the specified temperature in the sealed reactor vessel and was quantified using a pressure gauge positioned at the top of the reactor. A gas outlet and sampling valve were included to collect gas samples into a syringe for subsequent analysis.

The hydrothermal liquefaction procedure for biomass involved weighing the biomass feedstock and water, which were then introduced into the reactor in varying ratios (1:5 and 1:10 w/w) to examine the influence of the feedstock-to-water ratio on the characteristics of the resultant bio-oil. The single-step process under subcritical conditions was examined at various temperatures (250–350 °C) and residence durations (30 or 60 min). In single-step hydrothermal liquefaction under supercritical water conditions, the reactor was elevated to a temperature of 400 °C with varying residence lengths of 30 min or 60 min. The sequential two-step procedure involved initially heating the reactor to either 250 °C or 350 °C for a residence duration of 30 or 60 min, followed immediately by heating to supercritical water conditions at 400 °C for varying residence times of 30 or 60 min.

Upon loading the biomass and water into the reactor, it was sealed and purged with nitrogen to eliminate oxygen from the reactor. Following to each experiment, the reactor was extracted from the furnace and swiftly cooled using compressed air. The ultimate internal temperature and pressure were recorded and resulting gases were extracted under the pressure of the generated gases into a gas syringe for future compositional analysis. The reactor was subsequently opened and washed with 50 ml of dichloromethane (DCM) to remove the bio-oil from the solid byproduct (biochar). Vacuum filtering was employed to segregate the solid and liquid phases of the product. The solid product (biochar) was dehydrated at 105 °C until it attained a consistent weight in an oven. The liquid phase divides into two layers, and a decantation method was employed to isolate the aqueous phase product and bio-oil. The utilization of a closed autoclave batch reactor facilitated exceptional mass balances, achieving almost 100 % mass closure. The highest standard deviation of the product yield is approximately 0.001–0.01 (less than 1.0).

2.3. Gas analysis

The product gases were analysed with two distinct Varian 3380C gas chromatographs (GC). H_2, O_2, N_2, CO_2, and CO were examined by using a Varian gas chromatograph equipped with a packed column (2 m in length and 2 mm in diameter) containing a 60–80 mesh molecular sieve, employing argon as the carrier gas and thermal conductivity detection. Hydrocarbon gases were examined using a second Varian gas chromatograph use an 80–100 mesh Haysep packed column (2 m in length and 2 mm in diameter), with nitrogen as the carrier gas and flame ionisation detection. Gas standards were employed for calibration and identification, as well as for calculating the response factors. The gas

samples were tested in triplicate, and the average was employed to determine the individual gas volumetric concentration, as well as to calculate the molar concentration, volume percentage, and mass percentage utilising the Ideal Gas Law. The standard variation of gas analysis is approximately 0.02–0.9, which is more than the standard deviation of product yield yet remains below 1.0, signifying remarkable repeatability.

2.4. Oil analysis

The oil product obtained from the reactor through the extraction of bio-oil from biochar was evaluated via GC/FID (gas chromatography-flame ionisation detection) with a Varian 430-GC, with hydrogen provided by a QL-300A Hydrogen Generator. The column oven was set to 187 °C, while the oven temperature was maintained at 280 °C. The amounts of compounds discovered in the bio-oil were determined using a single external standard for each functional group. The identification of chemicals was confirmed using coupled gas chromatography-mass spectrometry utilising a Varian 3800-GC and Varian Saturn 2200 ion trap tandem mass spectrometer GC-MS/MS system, with the oven temperature set at 280 °C. GC/FID analysis up to 280 °C was found to cover the majority of the bio-oil components, with the 40 largest peaks in a representative sample corresponding to ≈89 % of the total oil mass. Compounds were identified using a series of conventional aliphatic, aromatic, and oxygenated compounds, supplemented by Kovats and Lee retention indices and the National Institute of Standards and Technology (NIST) chemical library [19,20]. The standard deviation of the bio-oil compositional analysis varied from 0.03 to 1.0.

2.5. Aqueous phase analysis

The aqueous phase obtained from the vacuum filtration process was analysed using an Agilent 1100 HPLC system (Zorbax Eclipse VDB-C8, Reverse Phase) equipped with a UV–Visible detector to quantify five groups of compounds: benzene derivatives (benzene and toluene), phenol derivatives (phenol, *m*-cresol, and *o*-cresol), organic acids and furfural derivatives (acetic acid, formic acid, furfural, guaiacol, and furan), and polycyclic aromatic hydrocarbons (naphthalene, phenanthrene, fluoranthene, fluorene, and pyrene). Each compound group was analysed using a specific method, which included tailored mobile phase composition, mobile phase flow rate, sample injection volume, oven temperature, and detection wavelength as shown in Table 1. The peak area of each detected compound was quantified using a calibration curve constructed for the corresponding compound, allowing for accurate determination of its concentration. A calibration curve was developed for each compound to produce the relation between the % area and standard compound concentration.

Table 1
Analytical conditions for the aqueous phase analysis by HPLC.

Acetic acid, Formic acid, Furfural, Guaiacol, and Furan	
Method:	
a. Mobile phase	A = Acetonitrile
b. Flowrate composition	B = 60 % Methanol in water
c. Flowrate	Isocratic with 35 % mobile phase B
d. Injection volume	1 ml/min
e. Temperature	10 μL
f. Wavelength	30 °C
	210 nm
Benzene and Toluene	
Method:	
a. Mobile phase	60 % Methanol in water
b. Flowrate composition	Isocratic
c. Flowrate	1 ml/min
d. Injection volume	25 μL
e. Temperature	35 °C
f. Wavelength	254 nm
Phenol, m-cresol, and o-cresol	
Method:	
a. Mobile phase	A = 0.1 % Formic acid in Acetonitrile
b. Flowrate composition	B = 0.1 % Formic acid in Water
c. Flowrate	Gradient
d. Injection volume	0.4 ml/min
e. Temperature	40 μL
f. Wavelength	25 °C
	280 nm
Naphthalene, Phenanthrene, Fluoranthene, Fluorene, Pyrene	
Method:	
a. Mobile phase	A = Acetonitrile
b. Flowrate composition	B = Water
c. Flowrate	Gradient
d. Injection volume	1.8 ml/min
e. Temperature	10 μL
f. Wavelength	27 °C
	280 nm

Table 2
Hydrothermal liquefaction of biomass in a one-step process under either subcritical or supercritical water reaction conditions in relation to process conditions.

One-step hydrothermal liquefaction conditions			Product yield		
Biomass to water ratio	Reaction Temperature	Reaction Time	Bio-oil	Biochar	Gas
(w/w)	(°C)	(min)	(w.%)	(wt.%)	(wt. %)
1:10	250	30	17.40	52.38	16.41
1:10	350	30	17.45	50.77	19.41
1:10	350	60	19.06	48.72	14.76
1:10	400	30	20.75	41.99	32.52
1:5	250	60	19.46	53.06	13.88
1:5	350	30	20.87	51.04	13.19
1:5	350	60	22.70	49.95	12.21
1:5	400	60	21.53	38.49	36.89

3. Results and discussion

3.1. Product yield

3.1.1. Product yield from one-step hydrothermal liquefaction of biomass

Table 2 presents the product yield from the one-step hydrothermal liquefaction of biomass, comparing experiments conducted with a 1:10 biomass to water ratio and a 1:5 biomass to water ratio under varying process conditions. The experimental process conditions examined intensify, progressing from subcritical hydrothermal liquefaction at 250 °C and 350 °C to supercritical water reaction conditions at 400 °C. In both the 1:10 and 1:5 biomass-to-water ratio tests, raising the harshness of the reaction conditions by elevated temperature and/or prolonged reaction residence time resulted in an increased bio-oil output. Under subcritical conditions, a maximum bio-oil production of 22.70 wt% was attained with a biomass to water ratio of 1:5 (w/w), a reaction temperature of 350 °C, and a reaction duration of 60 min. This suggests that increased biomass concentration, elevated temperature, and extended reaction duration facilitate the degradation of lignocellulosic constituents, thus augmenting bio-oil production [21,22]. It has been reported that a higher biomass concentration provides a greater quantity of lignocellulosic feedstock (primarily lignin, hemicellulose, and cellulose), which serves as the precursor for bio-oil formation [23]. In combination with higher reaction temperatures and prolonged residence times, this facilitates more effective depolymerization and conversion of biomass into hydrothermal liquefaction products [24,25]. Higher temperatures increase bio-oil and gas yields, while lower temperatures favour the formation of the aqueous phase and biochar [26]. Therefore, increasing the temperatures from subcritical to supercritical

conditions generally enhances bio-oil production.

The biochar obtained from the hydrothermal liquefaction process presents significant valorisation potential. Higher temperatures improve its quality by increasing fixed carbon and reducing volatile matter, although yields decline [27]. Such changes are linked to repolymerization and char-like structure formation, which enhance stability [28]. Process variables like temperature and residence time also affect bulk density, influencing its role in soil aeration, porosity, and microbial activity [29]. Biochar applications in soil can reduce compaction, improve water retention, and support crop yields under drought conditions [30]. Beyond agriculture, biochar versatility extends to catalysis, water treatment, carbon sequestration, and renewable energy [31], reinforcing its importance for the economic viability of hydrothermal liquefaction-based biorefineries.

At higher biomass concentration (biomass-to-water ratio of 1:5 w/w), Table 2 shows that the bio-oil yield is higher than that produced at the biomass: water ratio of 1:5 compared with the bio-oil yield at a biomass: water ratio of 1:10. Table 2 shows that increasing the temperature and/or the reaction residence time led to a decrease in biochar production at both 1:10 and 1:5 biomass: water ratios. Supercritical conditions are generally favourable for enhancing bio-oil production, provided that operational parameter (e.g., biomass concentration and mixing) are properly optimized. Therefore, a two-stage hydrothermal liquefaction strategy is proposed to maximize bio-oil yield. The subcritical stage facilitates the partial breakdown and preparation of biomass, while the subsequent supercritical water stage promotes efficient conversion and product yield enhancement [25]. It has been reported that higher hydrothermal liquefaction temperatures increase isomerization, depolymerization, and repolymerization of organic compounds within the biomass, causing bio-oil to be formed [32].

3.1.2. Product yield from the sequential two-step hydrothermal liquefaction of biomass

Table 3 shows the two-step hydrothermal liquefaction process results, whereby the biomass undergoes hydrothermal liquefaction involving a first step subcritical liquefaction investigated at different reaction temperatures and residence times followed directly by further processing under supercritical water liquefaction at a temperature of 400 °C and different residence times (30 min or 60 min). The highest bio-oil yield (25.44 wt%) was achieved at a biomass-to-water ratio of 1:10 (w/w), with process conditions at the first step of 250 °C for 30 min (subcritical) followed by 400 °C for 60 min (supercritical) at the second step. Optimal bio-oil production occurred when a shorter reaction time was used in the subcritical stage, followed by a longer reaction period at supercritical conditions. Elevated subcritical temperatures tend to reduce bio-oil yield. Moreover, higher biomass concentrations (e.g., 1:5 w/w) are not favourable due to char solidification, likely resulting from insufficient water [25,26,33]. Reaction time significantly influences hydrothermal liquefaction; a decreased reaction time enhances gas yield while decreasing bio-oil production. At 90 min, the bio-oil output markedly reduced across all temperatures. An increase in reaction time was noted to enhance the yield of bio-oil up to an ideal duration [32]. This restriction lowers the degree of biomass hydrolysis and the accessibility of intermediates necessary for bio-oil production. The optimal gas yield occurred at a biomass-to-water ratio of 1:10 (w/w), with both stages conducted at 250 °C and 400 °C for 60 min each. Gas production is improved by extended reaction durations and reduced biomass concentrations, which provide increased water availability. The increased water content facilitates the thermal decomposition of intermediate compounds into gaseous products [26]. The results show that the maximum biochar yield was obtained at a biomass-to-water ratio of 1:5 (w/w), using the two-stage process comprising 250 °C for 30 min (subcritical) followed by 400 °C for 30 min (supercritical). Biochar yield generally decreases with increasing temperature and prolonged reaction time. However, higher biomass concentrations contribute to elevated biochar yields due to the increased availability of lignocellulosic feedstock. Additionally, elevated biomass loading can lead to solidification and agglomeration of char, further increasing biochar formation [26]. Chopra et al. [34] also observed this tendency, demonstrating that the solid yield declined with increasing temperature, signifying a heightened conversion rate of biomass at elevated temperatures.

3.2. Bio-oil composition

3.2.1. Bio-oil composition from the one-step hydrothermal liquefaction of biomass

The composition of the bio-oil produced from the one-step and two-step hydrothermal liquefaction of biomass was determined using GC-MS and GC-FID techniques. Identified compounds were then categorized based on their functional groups [35]: (i) Hydrocarbons: saturated, unsaturated, aromatic (ii) Oxygenates: alcohols, aldehydes, ketones, acids, esters, ethers (iii) Phenolic compounds: phenols, alkylphenols, methoxyphenols (iv) Furans and derivatives (v) Nitrogen-containing compounds (vi) Sulphur-containing compounds (vii) Halogenated compounds (viii) Terpenoids/isoprenoids (ix) Naphthalene and polyaromatic hydrocarbon (PAH) derivatives (x) Miscellaneous/Unknowns.

Fig. 1 shows the bio-oil functional group composition for the one-step hydrothermal liquefaction of biomass at a 1:10 (w/w) in relation to various hydrothermal process conditions and Fig. 2 shows the 1:5 biomass to water ratio in relation to various process conditions. For the 1:10 biomass: water ratio, the greatest functional group that was contained in the bio-oil were phenols, oxygenates and furans derivatives at concentrations of 72.05 %, 22.61 %, 3.90 % respectively which comprises more than 98 % of the composition proportion.

No sulphur-containing compounds, naphthalene/PAH derivatives, or halogenated compounds were detected among the major peaks. Increasing reaction temperature led to a higher abundance of phenolic compounds, oxygenates, furans, and terpenoids [36], but decreased the proportion of hydrocarbons. A longer reaction time (from 30 min to 60 min) significantly increased the amounts of all functional groups, especially phenolic compounds and nitrogen-containing compounds, while decreasing the amount of terpenoid compounds [36]. However, compared to higher reaction temperatures applied over a shorter time, the longer reaction time resulted in a lower overall compound yield.

Nitrogen-containing compounds were more prevalent at longer reaction times (60 min), while terpenoids decreased in concentration

Table 3
Hydrothermal liquefaction of biomass in a two-step process of subcritical reaction followed directly by supercritical water liquefaction in relation to process conditions.

1st step conditions			2nd step conditions		Product yield		
Biomass to water ratio (w/w)	Reaction Temperature (°C)	Reaction Time (min)	Reaction Temperature (°C)	Reaction Time (min)	Bio-oil (wt.%)	Biochar (wt.%)	Gas (wt.%)
1:5	250	30	400	30	22.28	48.39	19.12
1:10	250	30	400	30	23.14	47.23	26.99
1:10	250	30	400	60	25.44	43.55	27.80
1:10	250	60	400	30	23.95	30.41	30.89
1:10	250	60	400	60	24.27	27.47	31.65
1:10	350	30	400	30	19.81	29.03	29.92

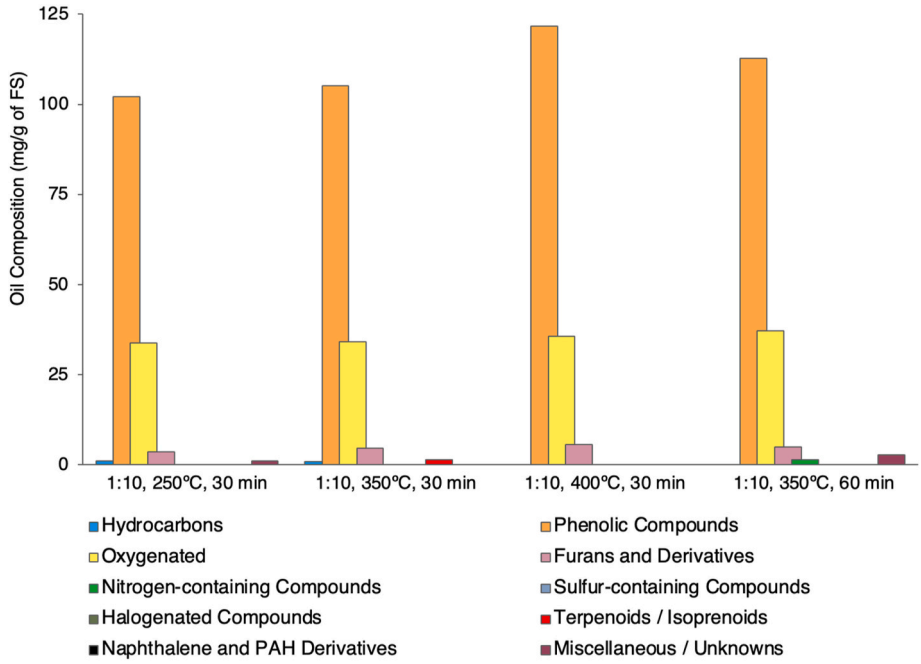

Fig. 1. Bio-oil functional group composition for one-step hydrothermal liquefaction of the feedstock biomass (FS) at a 1:10 biomass to water ratio in relation to various process conditions.

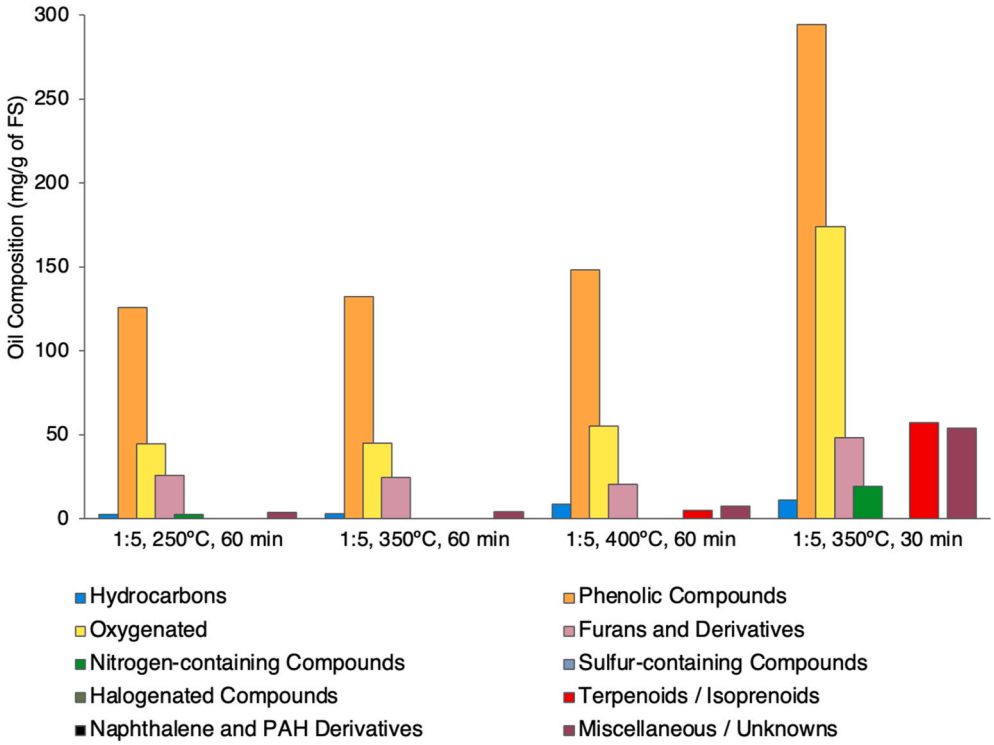

Fig. 2. Bio-oil functional group composition for one-step hydrothermal liquefaction of biomass at a 1:5 biomass to water ratio in relation to various process conditions.

under supercritical conditions (400 °C). The results showed that increasing the reaction temperature led to a decrease in nitrogen-containing compounds because nitrogen-containing compound preferentially dissolve into the aqueous phase [37], while a longer reaction time increased their presence but limited the variety of compounds formed. The main nitrogen-containing compounds were, 3-hydroxycarbofuran, carbamic acid, quinoline derivatives, nitrobenzaldehyde and indole derivatives. The nitrogen-containing compounds identified in the hydrothermal liquefaction bio-oil show differing degrees of precedence in the literature. Indole derivatives and quinoline-type N-heterocycles are among the commonly reported products, especially from protein- or nitrogen-rich feedstocks, because they arise from amino-acid decomposition (e.g., tryptophan) and Maillard-type or pyridine/pyrrole precursor pathways [38,39]. By contrast, free carbamic acid is not typically

reported in hydrothermal liquefaction bio-oil: it is chemically unstable under hydrothermal conditions and is expected to decompose to CO_2 and ammonia, or else convert into more stable derivatives such as carbamates or amides [40,41]. Nitrobenzaldehyde and other nitro-aromatics are similarly unusual as hydrothermal liquefaction formation products. Nitration reactions require strong oxidizing or nitrating conditions, which are not characteristic of standard subcritical or supercritical water liquefaction; detection of nitro-substituted aromatics would therefore more likely reflect feedstock contamination, co-processing of waste streams containing nitro compounds, or spectral library mis-assignments [25]. 3-Hydroxycarbofuran is a known pesticide metabolite and not part of typical biomass decomposition reactions, and its presence in bio-oil would thus strongly suggest feedstock contamination with carbofuran or related carbamate pesticides rather than in situ hydrothermal liquefaction formation [41].

The increase in phenolic compounds, oxygenates, furans, and terpenoids with rising reaction temperature, accompanied by a reduction in hydrocarbons, can be attributed to the enhanced reaction kinetics under high-severity conditions. At elevated temperatures, the activation energy barriers for hydrolysis, depolymerization, and bond cleavage reactions are more readily overcome, thereby promoting the breakdown of macromolecules and facilitating the conversion of hydrothermal liquefaction intermediates into biocrude oil [42,43]. Such conditions favour the generation of oxygenated products, including phenols, furfurals, and nitrogenous derivatives, which are increasingly incorporated into the oil phase at higher severities [42,44]. Conversely, hydrocarbons are diminished due to enhanced cracking and rearrangement reactions, with excessive temperatures (>400 °C) further shifting product distributions toward char and gaseous phases [45,46]. Prolonging the reaction time from 30 to 60 min similarly intensifies secondary conversions, enabling interconversion among oil, aqueous, and solid phases and facilitating the stabilization of intermediates as phenolic and nitrogen-containing compounds [44,47,48]. However, because terpenoids are relatively volatile and chemically labile, extended thermal exposure promotes their degradation via cracking, oxidation, or rearrangement, thereby lowering their abundance in the product spectrum. These observations are consistent with the general trend that increasing temperature and residence time synergistically drive the transformation of transient intermediates toward more stable aromatic and heteroatom-containing compounds [49].

In relation to the results from the 1:5 biomass to water ratio (Fig. 2), the higher concentration of biomass showed that the highest functional group compounds found in the bio-oil were phenols, oxygenates and furan derivatives at 53.24 %, 25.54 %, 8.01 % respectively which comprised more than 85 % of the total composition proportion. Increasing biomass concentration resulted in higher yields across all the functional groups. As with the 1:10 biomass: water ratio product bio-oil, no sulphur-containing compounds, naphthalene/PAH derivatives, or halogenated compounds were observed among the major components. At the biomass to water ratio of 1:5 (w/w), increasing the reaction temperature enhanced the quantity of almost all functional groups, except furans and their derivatives (Fig. 2). The increase in the functional groups ranged from approximately 4 %–199 %. Moreover, a shorter reaction time (30 min) resulted in the highest functional group yield compared to all compounds produced at a reaction time of 60 min, even under higher temperatures.

The compounds observed in the product bio-oil were classified according to their respective carbon number distribution. The outcomes for the liquefaction of biomass using subcritical and supercritical water at a biomass to water ratio of 1:10 are illustrated in Fig. 3(a) and (b), respectively, at a water to biomass ratio of 1:10 (w/w). Light hydrocarbons within the C5 – C9 range were the predominant fraction of the bio-oil, representing approximately 96.30 % of the overall composition. The C5 – C9 fraction, representative of the standard carbon chain length in gasoline, was prevalent, succeeded by the C10 – C15 and C12 – C20 fractions.

At a biomass-to-water ratio of 1:5 (w/w), Fig. 4 shows that the hydrocarbon composition remained primarily dominated by the C5 – C9 range. However, an observable increase in the proportion of longer-chain hydrocarbons, specifically within the C10 – C15 and C12 – C20 ranges, was noted. This shift indicates that higher biomass concentrations tend to promote the formation of longer hydrocarbon chains in the bio-oil, while simultaneously reducing the fraction of shorter-chain compounds (C5 – C9). A biomass-to-water ratio of 1:5 (w/w) was found to promote the formation of longer hydrocarbon chains in the resulting bio-oil compared to a ratio of 1:10 (w/w) (Fig. 4). This trend may be attributed to the increased feedstock loading, which provides a greater availability of carbon-rich compounds for chain growth. Additionally, experiments conducted at the 1:5 (w/w) ratio were performed with extended reaction times (60 min), which likely facilitated further polymerization and secondary reactions, contributing to the formation of longer hydrocarbon chains.

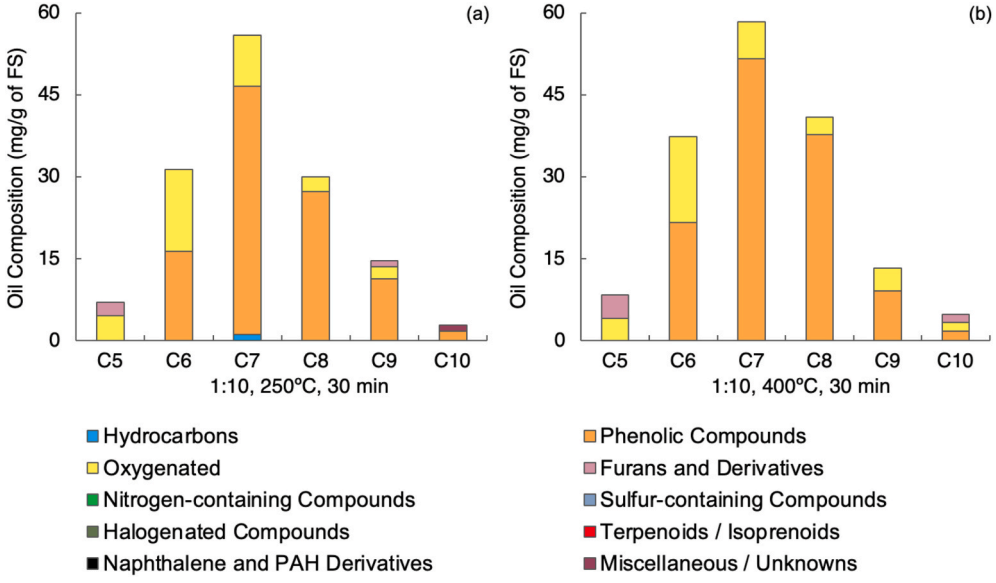

Fig. 3. Relative carbon number distribution in the bio-oil produced via one-step (a) subcritical water and (b) supercritical water liquefaction of biomass at the biomass:water ratio of 1:10 (30 min residence time).

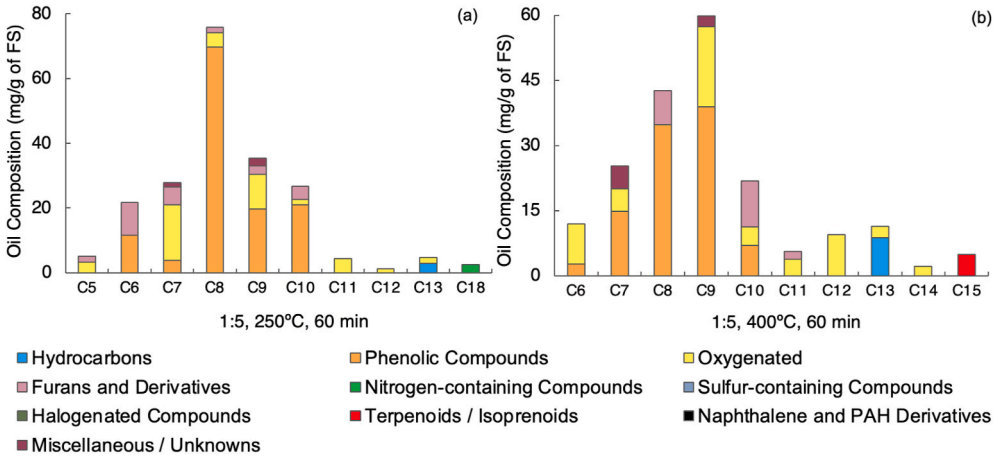

Fig. 4. Relative carbon number distribution in the bio-oil produced via one step (a) subcritical water and (b) supercritical water liquefaction of biomass at the biomass:water ratio of 1:5 (60 min residence time).

3.2.2. Bio-oil composition from the sequential two-step hydrothermal liquefaction of biomass

The bio-oil obtained from the two-stage hydrothermal liquefaction of biomass was investigated concerning the process parameters of temperature and reaction duration in either the first or second step of the two-step process. The findings are illustrated in Fig. 5. The functional groups in the bio-oil produced from the two-step method were largely oxygenates, phenolic compounds, and furans and their derivatives. Fig. 5 indicates that the content of hydrocarbons in the resultant bio-oil escalated with prolonged reaction time and elevated biomass concentration. Also, greater quantities of hydrocarbons were formed at elevated reaction temperatures under subcritical conditions. Phenolic chemicals also elevated with increased temperatures at subcritical conditions and larger biomass concentrations.

Oxygenates increased with longer reaction time, higher reaction temperature in subcritical conditions, and higher biomass concentration (Fig. 5). Furans and derivatives also increased with higher temperatures in subcritical conditions and higher biomass concentration. Nitrogen-containing compounds increased with higher biomass concentration and higher reaction temperature and terpenoids/isoprenoids increased in concentration in the bio-oil with longer reaction time, higher reaction temperature, and higher biomass concentration.

The increase in oxygenated compounds with higher reaction temperature, longer residence time, and elevated biomass concentration is primarily associated with hydrolysis and depolymerization of polysaccharides, followed by dehydration and fragmentation reactions. Under subcritical water conditions, the enhanced ionic product facilitates hydrolytic cleavage of glycosidic and ester linkages, leading to the formation of carbohydrate intermediates such as cello-oligomers, glyceraldehydes, and furfurals, many of which dissolve into the aqueous fraction before progressively partitioning into the oil phase as oxygenates at longer retention times [42,44,48]. With increasing temperature, the activation energy barrier for dehydration and cyclization reactions is more easily overcome, thereby promoting the accumulation of furanic compounds and their derivatives [50,51].

The abundance of nitrogen-containing compounds at higher severity is linked to the thermal degradation of proteins and nucleic acids, releasing amino acids, amides, and heteroaromatic derivatives, which are incorporated into the biocrude phase with increasing temperature and biomass loading [44,49,52]. Similarly, longer retention times enhance interconversion between aqueous, oil, and solid fractions, enabling nitrogenous intermediates to undergo secondary reactions and stabilization as heteroaromatic compounds [48,53].

The compounds in the bio-oil resulting from the two-step sequential subcritical and supercritical hydrothermal liquefaction of biomass were characterised based on carbon number (Fig. 6). Compared to one-step hydrothermal liquefaction (Figs. 3 and 4), the two-step process yields a higher proportion of longer carbon number compounds. This suggests that the extended overall reaction time in the two-step process enhances the thermal breakdown and transformation of lignocellulosic biomass

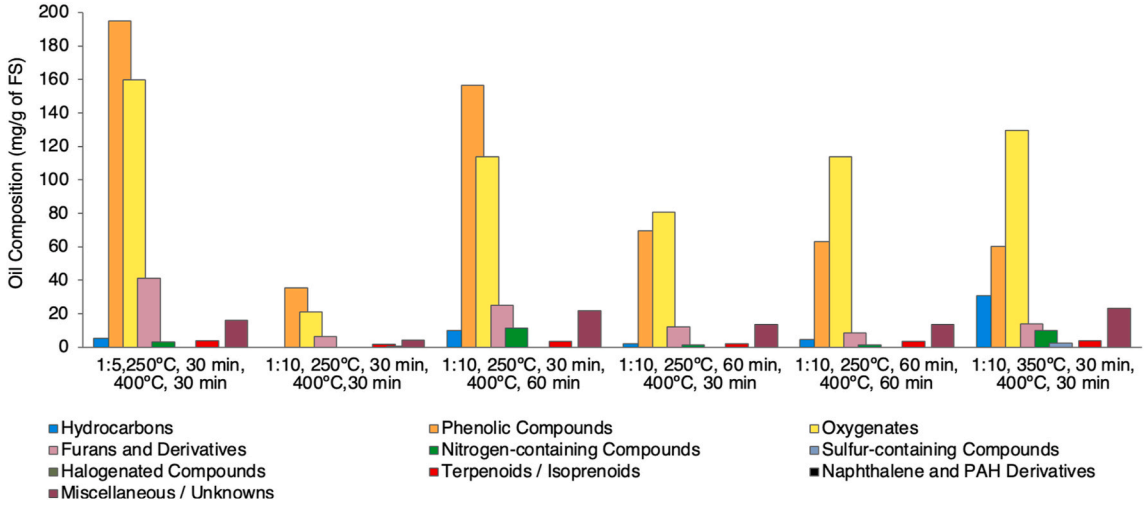

Fig. 5. Bio-oil functional group composition for the two-step hydrothermal liquefaction of biomass in relation to various process conditions.

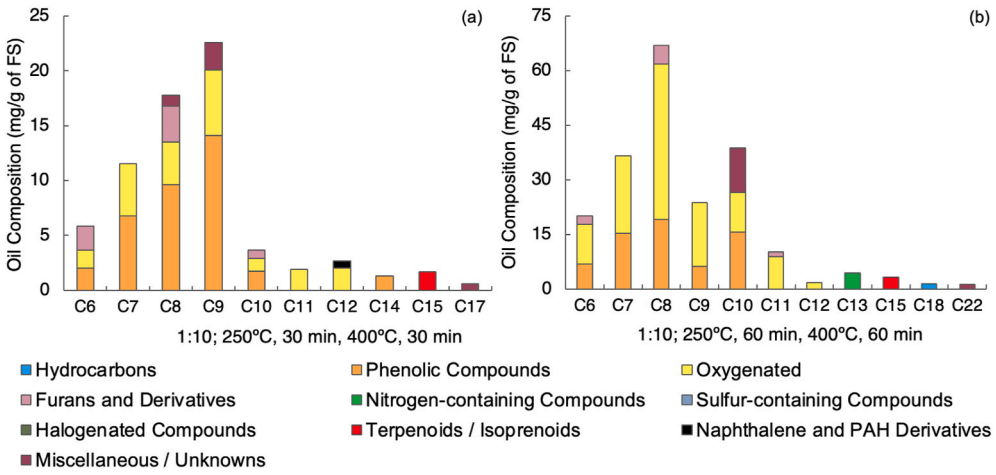

Fig. 6. Relative carbon number distribution in the bio-oil produced via two-step sequential subcritical water and supercritical water liquefaction of biomass at the biomass:water ratio of 1:10 (a) 30 min residence time (b) 60 min residence time at each step.

into more complex and heavier hydrocarbon structures. The increased presence of longer carbon number compounds indicates enhanced polymerization and secondary reactions occurring during the second, supercritical water reaction stage. Furthermore, the longer carbon number fractions (C10–C20) in the two-step process contain significant amounts of nitrogen-containing compounds. This suggests that nitrogenous components in the biomass, such as proteins or amino acids, contribute significantly to the formation of complex molecules under two-stage processing conditions.

The results indicate that the two-step hydrothermal liquefaction process offers distinct advantages over the one-step approach, including improved bio-oil yield and enhanced oil quality. These findings suggest that the second thermal stage facilitates further depolymerization and partial stabilization of intermediate compounds, leading to more favourable product characteristics. However, the absence of a catalyst limits the extent of deoxygenation and may result in higher aqueous-phase formation compared to catalytic hydrothermal liquefaction reported in the literature.

Catalytic hydrothermal liquefaction has been widely studied for improving bio-oil yield and quality. Various catalysts, such as heterogeneous metal catalysts (e.g., Co/CNTs, Ni, Ru) or acidic zeolites (HZSM-5), have been shown to significantly influence both yield and chemical composition. For example [54], reported that Co/CNTs increased bio-oil yield and conversion to 40.25 wt% and 95.78 %, respectively, while producing bio-oil with a higher hydrocarbon content and lower fatty acid content. Similarly, Ma et al., [55] observed that heterogeneous catalysts slightly increased bio-oil yield and enhanced HHV by approximately 10 % compared to non-catalytic hydrothermal liquefaction.

Catalyst type, loading, and composition are critical for product quality. Duan and Savage [56], reported that catalysts improve HHV and lower the O/C ratio, while combinations of catalysts may provide synergistic effects, although detailed mechanisms remain under investigation. Commercially abundant catalysts with large surface areas are attractive for industrial applications due to their effectiveness and ease of recycling [57].

While this study focuses on non-catalytic one-step and two-step hydrothermal liquefaction, the comparison with literature catalytic hydrothermal liquefaction underscores the potential benefits of integrating catalysts in future work. Non-catalytic two-step hydrothermal liquefaction provides a clear baseline, showing that process design alone can improve product characteristics, but catalytic interventions are expected to further enhance bio-oil yield and quality. Preliminary experiments with catalytic two-step hydrothermal liquefaction are planned to directly evaluate these improvements.

3.3. Gaseous product composition

The gas product composition was analysed by packed column gas chromatography, revealing that both the one-step and two-step processes predominantly yielded CO and CO_2, with the residual fraction comprising hydrogen, methane, propane, propene, ethane, ethene, butene, and butadiene as shown in Figs. 7 and 8.

3.3.1. Gas composition from the one-step hydrothermal liquefaction of biomass

The composition of product gases resulting from the one-step hydrothermal liquefaction of biomass, corresponding to biomass-to-water ratios of 1:10 and 1:5, is illustrated in Fig. 7(a) and (b), respectively. The gas composition resulting from the one-step hydrothermal processing of biomass at a 1:10 biomass-to-water ratio is predominantly CO, whereas at a higher biomass concentration of 1:5, CO_2 emerges as the principal gas component. Lu et al. [58] similarly reported findings from the hydrothermal liquefaction of sewage sludge. This signifies that water produces CO via water-gas shift interactions [24,37]. Extended retention durations elevate H_2, CO_2, CH_4, C_2, and C_3, while diminishing CO and C_4. Moreover, elevating the reaction temperature enhances the production of all gaseous chemicals [24,59]. Previous observations have indicated that the gas phase containing higher hydrocarbons increases with rising temperature [60].

Furthermore, the production of other gaseous species, such as CH_4 and H_2, can be linked to secondary cracking, reforming, and hydrogenation reactions occurring in both one-step and two-step hydrothermal liquefaction processes [45,49]. These reactions collectively illustrate the mechanistic basis for the observed gas distribution and its relationship to bio-oil quality, demonstrating that gas-phase reactions not only serve as indicators of biomass conversion severity but also actively influence the reduction of oxygen-containing compounds and the enrichment of energy-dense, stable products in the liquid phase.

3.3.2. Gas composition from the sequential two-step hydrothermal liquefaction of biomass

Fig. 8 illustrates the gas composition generated from the two-step hydrothermal liquefaction of biomass, initially utilising subcritical water followed by supercritical water processing, in relation to the varying process conditions at both stages. The gases generated are mostly carbon dioxide, methane, carbon monoxide, and hydrogen. Elevating the reaction temperature under subcritical circumstances (from 250 °C to 350 °C) augments the yield of all gaseous chemicals, as confirmed by Zhu et al. [61] in their study on the hydrothermal liquefaction of biomass (barley straw). The elevated temperature and

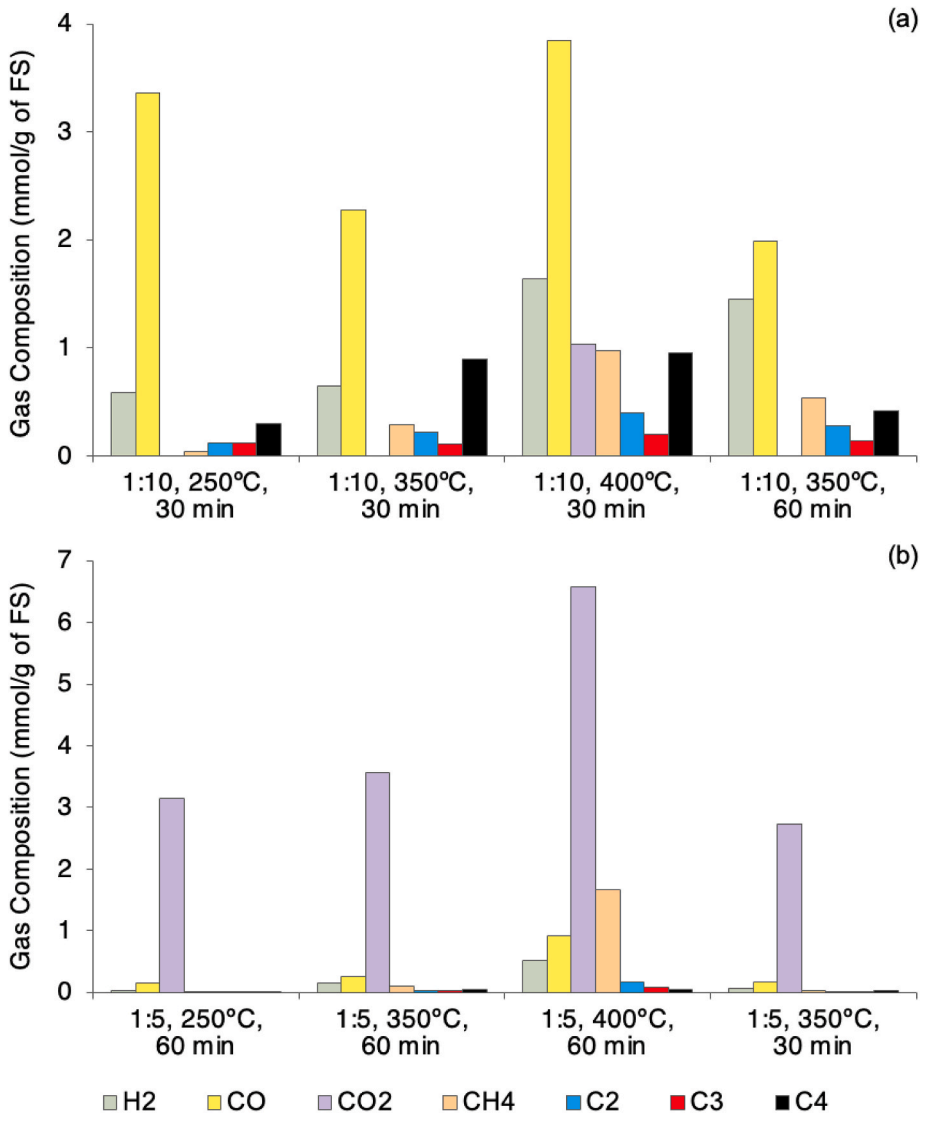

Fig. 7. Gas composition for one-step hydrothermal liquefaction of biomass in relation to various process conditions (a) 1:10 biomass:water ratio (b) 1:5 biomass: water ratio.

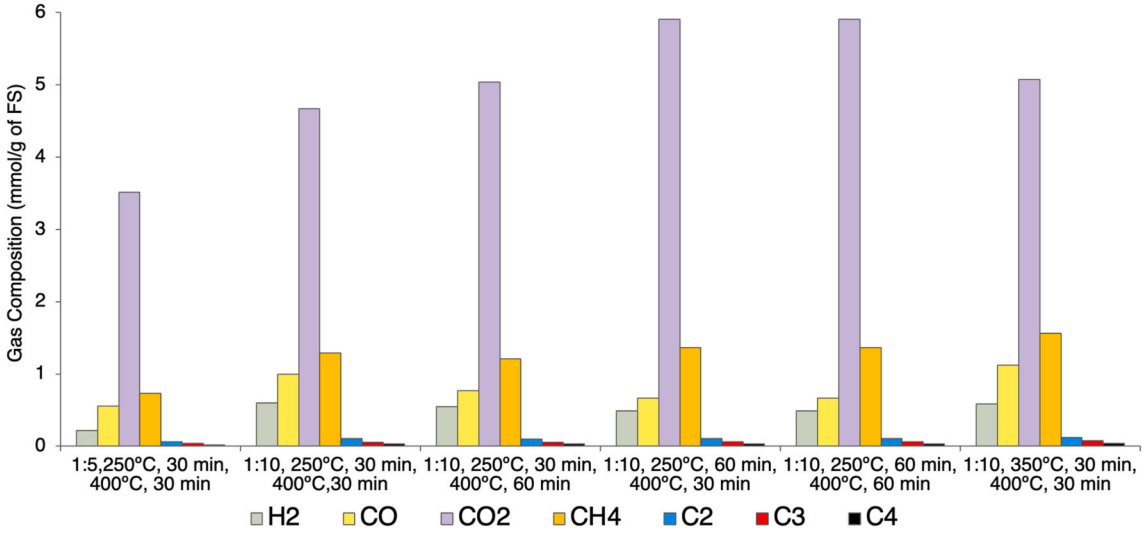

Fig. 8. Gas composition produced via two-step sequential subcritical water and supercritical water liquefaction of biomass in relation to process conditions.

extended residence time of hydrothermal liquefaction promote the breakdown of hydrolysed organic molecules into CO and CO_2 [62]. Conversely, increased biomass concentration diminishes gas production, as evidenced by the biomass-to-water ratio of 1:5 depicted in Fig. 8. A reduced biomass concentration delivers additional water into the hydrothermal liquefaction process, potentially resulting in enhanced gas production [63]. The CO_2 yield markedly increased in the gas product from the two-step hydrothermal liquefaction method, suggesting that the water-gas shift reaction is thermodynamically favoured under elevated temperature settings and extended reaction durations [59].

In addition to the water-gas shift (WGS) reaction, which converts CO and H_2O to CO_2 and H_2, carbon monoxide can also be generated via decarbonylation reactions, in which carbonyl groups are cleaved from biomass intermediates under hydrothermal conditions [42,51]. These decarbonylation reactions contribute significantly to the observed CO yield and represent a parallel pathway to WGS in subcritical and near-supercritical water. Carbon dioxide formation similarly arises from both the WGS reaction and decarboxylation, in which carboxyl groups are removed from oxygenated intermediates, resulting in the release of CO_2 while simultaneously reducing the oxygen content of the biomass-derived molecules [44,52].

3.4. Aqueous phase composition

The hydrothermal liquefaction process involves water which acts as a reactant and as a solvent to breakdown lignocellulosic biomass into bio-oil and other chemicals. At subcritical conditions, the water not only acts as a solvent but also catalyses chemical reactions [61,64,65]. Previous studies indicate that approximately one third of the organic carbon in the feedstock is transferred to the aqueous phase during hydrothermal liquefaction, suggesting that hot and pressurised water can decompose biomass during this process [37,66]. The aqueous phase offers the potential for recycling and reuse owing to its high organic content [67].

The aqueous phase obtained from biomass for both the direct one-step and the two-step subcritical followed by supercritical water processing was analysed for various compounds that reflect the thermochemical degradation of the lignocellulosic biomass. Identified compounds include: (i) Carboxylic acids: acetic acid, formic acid; (ii) Furan derivatives: furfural, furan; (iii) Phenolic compounds: guaiacol, phenol, *m*-cresol, *o*-cresol: (iv) Aromatic compounds and PAHs: benzene, toluene, naphthalene, phenanthrene, fluoranthene, pyrene, fluorine. These compounds signify the degradation of the three principal constituents of lignocellulosic biomass: cellulose, hemicellulose, and lignin, during the hydrothermal liquefaction process [35,68,69].

In all aqueous phase samples, acetic acid was the predominant component resulting from both direct and two-stage hydrothermal liquefaction [35]. The elevated content indicates the significant decomposition of lignocellulosic material. Acetic acid is produced by the decomposition of cellulose, hemicellulose, proteins, and lipids [70]. Zhu et al., [68] similarly discovered that acetic acid constituted the predominant species, comprising over 24 % of the whole examined sample. Xylan, a predominant hemicellulose, possesses acetyl side chains that are liberated as acetic acid after hydrolysis [68]. This highlights the capacity of the hydrothermal liquefaction technique to degrade lignin while simultaneously hydrolysing hemicellulose and cellulose, thus facilitating acetic acid production. Moreover, acetic acid is a comparatively persistent intermediate under hydrothermal liquefaction conditions, which presumably accounts for its abundance in the aqueous phase.

3.4.1. Aqueous phase composition from the one-step hydrothermal liquefaction of biomass

Fig. 9 shows the composition of the aqueous phase derived from the one-step hydrothermal liquefaction in relation to process conditions in relation to a 1:10 biomass: water ratio for acetic acid (Fig. 9(a)) and also other major compounds (Fig. 9(b)). Fig. 9(c) and (d) shows the results for the 1:5 biomass: water ratio for acetic acid and other major compounds respectively. The generation of essential intermediates and

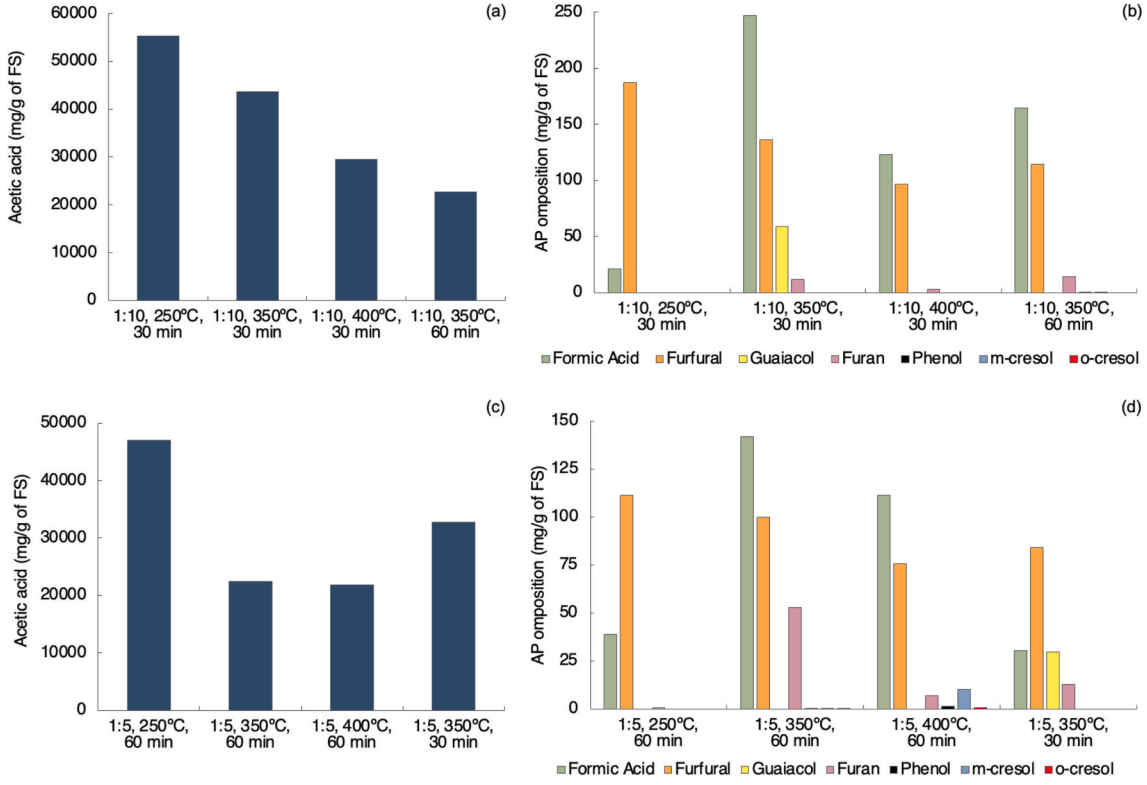

Fig. 9. Aqueous phase composition from the one-step hydrothermal liquefaction in relation to process conditions (a) acetic acid with 1:10 biomass: water ratio (b) other major compounds with 1:10 biomass: water ratio (c) acetic acid with 1:5 biomass: water ratio (d) other major compounds with 1:5 biomass: water ratio.

products demonstrated distinct correlations with reaction temperature, residence duration, and biomass concentration. In the aqueous phase composition at a 1:10 biomass to water ratio, the concentration of acetic acid exhibited a decreasing trend with elevated reaction temperatures and extended reaction durations (Fig. 9(a)). Higher biomass loading (1:5 w/w) promoted higher yields of acetic acid (Fig. 9(c)). In contrast, formic acid displayed a temperature-dependent dual behaviour, increasing under subcritical conditions but decreasing at supercritical temperatures (400 °C). Its formation was further enhanced under lower biomass concentrations (biomass:water ratio 1:5) and shorter reaction times, suggesting that formic acid is favoured under milder hydrothermal conversion conditions. Furfural production decreased with both increasing temperature and reaction time, and its concentration was similarly reduced at higher biomass loading, indicating its susceptibility to secondary degradation under harsher conditions.

Furan derivatives were mainly detected at temperatures above 350 °C, with furan yields increasing at extended reaction times and higher biomass concentrations. Nevertheless, further temperature elevations resulted in decreased furan concentrations, presumably attributable to thermal breakdown or repolymerization mechanisms. The synthesis of phenolic chemicals, such as phenol, guaiacol, m-cresol, and o-cresol, was limited to elevated temperatures (>350 °C), with phenol and cresols appearing only after extended reaction durations (60 min). Notably, higher biomass concentrations generally suppressed phenolic compound yields, while guaiacol was detected only at 350 °C with a short reaction time of 30 min, suggesting that it is an intermediate rapidly converted under harsher reaction conditions.

These results collectively suggest that product distribution is strongly governed by the balance between depolymerization, dehydration, and secondary decomposition reactions. At moderate conditions, primary degradation products such as formic and acetic acids dominate, while elevated temperatures and prolonged reaction times promote secondary pathways, leading to the degradation of furanic and phenolic intermediates [62]. Formic acid derives from the rehydration of 5-HMF and is present both in cellulose and lignin which can also degrade to acetic acid [62,71]. Acetic acid is formed from the fragmentation of fructose, which involves the decarboxylation or decarbonylation of lactic acid, produced from the oxidation of acetaldehyde obtained from glucose, as well as the oxidation of HMF and furfurals [72–74]. Furan and furfural derivatives derived from sugar degradation sourced from cellulose [25,75]. While phenolic derivatives are the main products of lignin decomposition. Phenol originates from the hydrolysis of lignin, involving the cleavage of β-O-4 ether bonds and C-C bonds, while other phenolic compounds derive from demethoxylation and alkylation reactions [76].

3.4.2. *Aqueous phase composition from the sequential two-step hydrothermal liquefaction of biomass*

In the two-step hydrothermal liquefaction process, Fig. 10(a) shows that acetic acid remained the predominant compound in the aqueous phase, followed by formic acid, furfural, guaiacol, furan, phenol, and cresols (Fig. 10(b)). Compared to the one-step hydrothermal liquefaction process, the two-step subcritical-supercritical process resulted in generally higher concentrations of these compounds, indicating that the combined subcritical–supercritical approach promotes enhanced chemical release and solubilization. Notable variations were observed in the behaviour of individual compounds when comparing two-step to one-step hydrothermal liquefaction. Guaiacol was detected exclusively

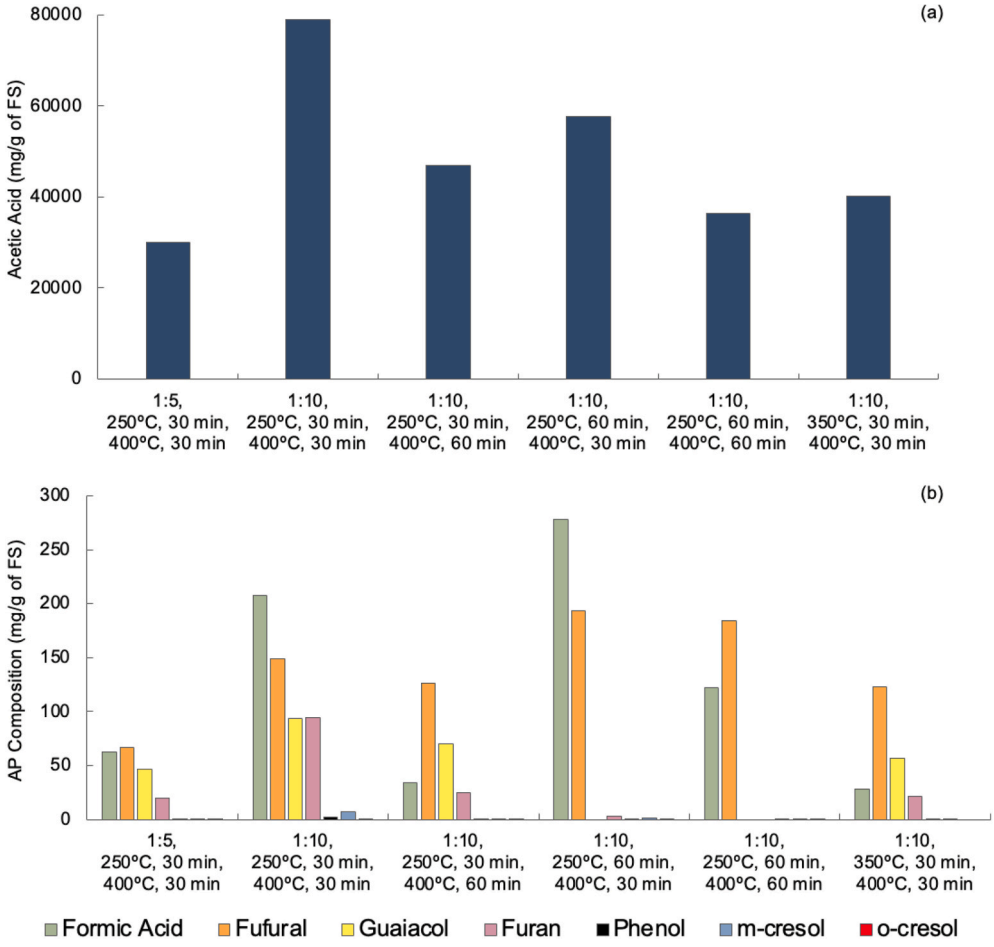

Fig. 10. Aqueous phase composition from two-step hydrothermal liquefaction of biomass in relation to process conditions (a) acetic acid (b) other major compounds.

at 30-min reaction times under subcritical conditions, with higher yields observed at shorter reaction times and lower subcritical temperatures.

Under subcritical temperatures (250–350 °C), hemicellulose and lignin partially depolymerize, releasing lower-molecular-weight intermediates such as formic acid, acetic acid, and guaiacol. Otherwise, supercritical conditions further promote solubilization and prevent the recondensation of these intermediates, resulting in increased aqueous-phase concentrations [77,78]. Specifically, guaiacol was detected only during reduced subcritical exposure (30 min), indicating its rapid formation and removal prior to recondensation into phenolic char at higher severity [75,79].

Furan formation primarily occurred at extended total reaction times of 60–90 min, but its concentration decreased with further increases in reaction time and biomass loading. Unlike direct hydrothermal liquefaction, phenol was also detected at lower subcritical temperatures (250 °C), and its concentration increased with rising subcritical temperatures while declining at longer reaction times and higher biomass concentrations. Both m-cresol and o-cresol were detected at 250 °C, the yield of m-cresol increased under shorter reaction times and lower biomass loadings, while o-cresol formation was enhanced at lower subcritical temperatures, shorter reaction times, and reduced biomass concentrations.

Phenol and cresols, which were also identified at 250 °C, exhibited yields that increased with subcritical temperature but were suppressed by extended reaction times and higher biomass concentrations, reflecting a balance between lignin-derived aromatic intermediate formation and secondary condensation or phase separation under crowding conditions [25,75]. During hydrothermal liquefaction, lignin undergoes depolymerization and cleavage of ether and C–C bonds, producing smaller phenolic intermediates such as phenol, guaiacol, and cresols [80–82]. Moreover, under harsher conditions (longer reaction times, higher biomass concentration), these phenolic intermediates can undergo re-condensation or polymerization into heavier, insoluble structures (such as char or tar) [83].

The aqueous phase derived from hydrothermal liquefaction of biomass contains a diverse array of organic compounds, including carboxylic acids (acetic acid, formic acid), furan derivatives (furfural, furan), and phenolic compounds (guaiacol, phenol, m-cresol, o-cresol). These constituents render the aqueous a promising feedstock for various industrial applications. For instance, carboxylic acids such as acetic and formic acids can be utilised in biochemical processes, serving as precursors for the synthesis of biodegradable plastics, solvents, and as intermediates in the production of biofuels [84]. Furan derivatives, including furfural, are valuable in the production of resins, agrochemicals, and as solvents in the chemical industry [85]. Phenolic compounds like guaiacol and cresols have potential applications in the pharmaceutical industry, as flavour and fragrance agents, and as precursors for high-value chemicals [86]. Moreover, the aqueous can be integrated into thermochemical conversion processes such as gasification, providing a route to bio-syngas or hydrogen, thereby enhancing the overall sustainability and economic viability of hydrothermal liquefaction-based biorefineries [43]. Valorising the aqueous phase in these manners contributes to the circular economy by maximizing the utilization of all biomass fractions.

3.5. Reaction mechanism

3.5.1. One-step reaction mechanism

The hydrothermal liquefaction process can be adjusted by altering the hydrothermal parameters, primarily reaction temperature, residence time, and biomass-to-water ratio. It can be employed to improve the yield and quality of the targeted co-products and biofuel [87]. Under hydrothermal liquefaction conditions, water exhibits a significant degree of solvation with organic substances, attributable to the change of its dielectric constant. Under hydrothermal liquefaction conditions, water diminishes its polarity, acquiring properties akin to organic solvents. The reaction mechanisms are precisely determined by the trajectory of a certain component, and to enhance comprehension of hydrothermal liquefaction, particular model compounds are typically selected.

The hydrothermal liquefaction process is intricate due to the complexity of lignocellulosic biomass, which comprises cellulose, hemicellulose, and lignin, each exhibiting distinct reaction mechanisms [88,89]. Depolymerization of lignocellulosic biomass entails the disintegration of monomers and the recombination of reaction intermediates, which constitute the majority of the hydrothermal liquefaction reaction processes. Lignocellulose undergoes depolymerization to yield monomers, fragmenting into smaller components via decomposition processes including cleavage, dehydration, and decarboxylation. These fragments experience cyclization, condensation, and repolymerization to yield hydrothermal products including bio-oil, aqueous phase, gas, and solid residues [90,91]. Hemicellulose is thermolabile at temperatures over 140 °C, resulting in the formation of xylose, arabinose, and galactose. The depolymerization or hydrolysis of macromolecules constitutes the initial phase of hydrothermal liquefaction. Macromolecules decompose into smaller molecules, such as carbohydrates into monosaccharides, lignin into phenols, proteins into amino acids, and lipids into fatty acids and glycerol. Consequently, hydrolysis products engage in several processes, including breakdown, dehydration, deamination, and decarboxylation, which occur as a result of elevated temperatures. Decomposition reactions transpire between a temperature range of 180–340 °C, with monosaccharides being the initial chemicals to degrade at 180 °C.

The solubilization and decomposition of proteins and lipids are observed at temperatures exceeding 200 °C, with complete decomposition occurring at temperatures above 300 °C. Recombination and repolymerization represent an additional reaction mechanism occurring at temperatures concurrent with the decomposition of monosaccharides. Highly reactive organic molecules undergo recombination above 300 °C, resulting in the formation of organic compounds such as ketones, aldehydes, amines, and hydrocarbons, which are found in the aqueous phase of the bio-oil [33,92]. The dehydration reaction pertains to the elimination of H_2O, whereas the decarboxylation reaction addresses the expulsion of carbon dioxide, and deamination involves the removal of amino acids [3]. In the hydrothermal liquefaction process, the removal of unsaturated oxygen occurs through the elimination of water or carbon dioxide, facilitated by transformation processes such as decarboxylation and dehydration [93].

The deficiency of hydrogen-induced reactions in the recombination and repolymerization of reactive fragments signifies the reversal of the initial processing phase [94]. Thus, the deficiency of hydrogen molecules or the surplus of larger free radicals promoted the recombination or repolymerization of lower molecular weight compounds, leading to the production of higher molecular weight compounds or the formation of coke. The hydrogen-rich organic matrix produced free radicals with highly stable molecular weight molecules [95].

3.5.2. Two-step hydrothermal liquefaction reaction mechanism

Hydrothermal reactions are both a heterogeneous and homogenous nature depending on the substrate [62]. The typical reactions that are involved are hydrolysis, decomposition, recombination and aromatization. Fig. 11 illustrates a two-step hydrothermal liquefaction process for converting lignocellulosic biomass into bio-oil. Two-step hydrothermal liquefaction involves subcritical condition for the 1st step and supercritical for the 2nd step. Each of the steps has specific goals, the 1st step focuses on depolymerization of the lignocellulosic matrix into smaller intermediates while the 2nd step focuses on the upgrading of the intermediates by decarboxylation, cracking, and aromatization to yield high-quality bio-oil.

Previously proposed processes have examined the two stages of the two-step hydrothermal liquefaction process concerning the primary biopolymers of lignocellulosic biomass: cellulose, hemicellulose, and

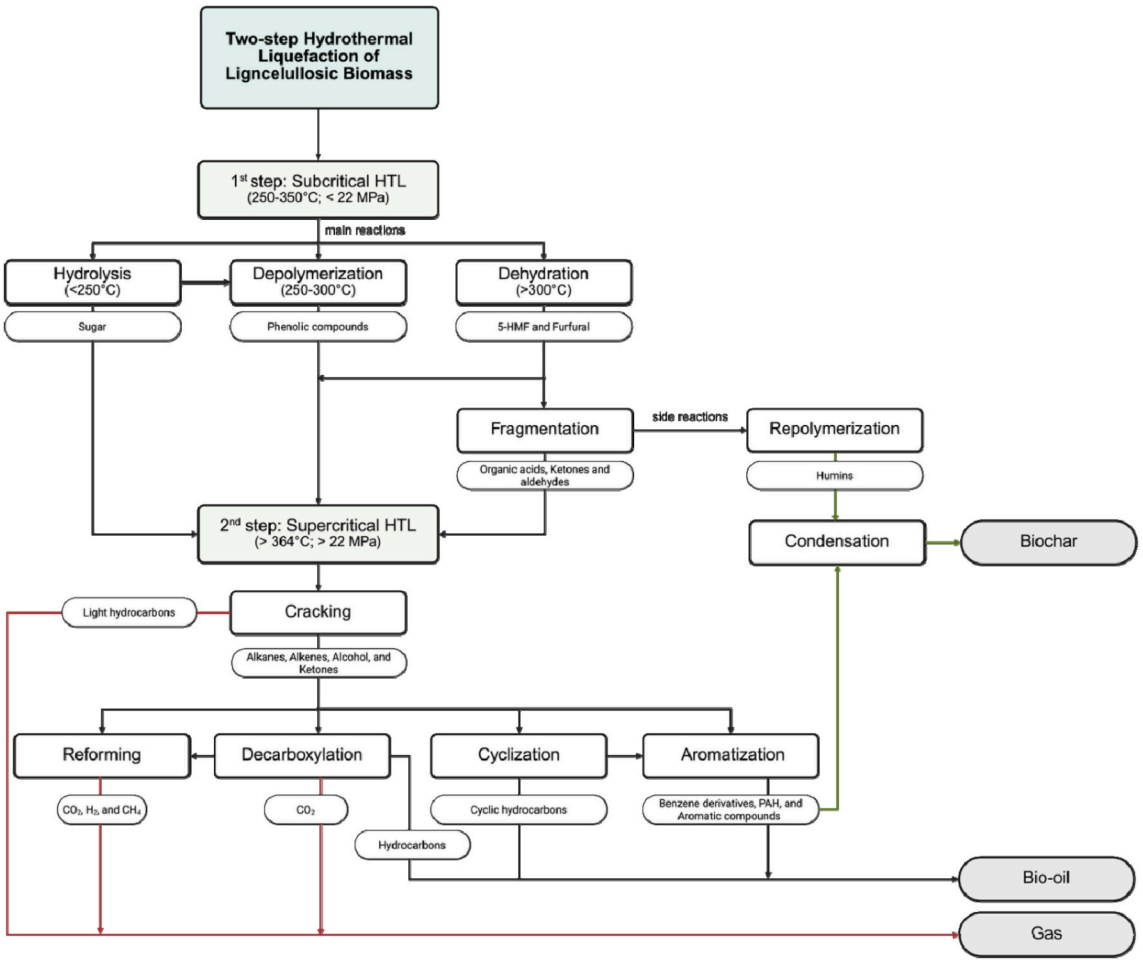

Fig. 11. Two-step hydrothermal liquefaction reaction mechanism.

lignin. For example, Tolenen [64]. Suggested for the two-step hydrothermal liquefaction of cellulose that initially hydrolysis produces, C_6 sugars (glucose, mannose, xylose), where the glycosidic bonds are cleaved by the high ionic product of subcritical water. The sugars such as glucose react via dehydration to produce 5-HMF and sugar derivatives react to form furan derivatives. Finally, fragmentation converts the 5-HMF to levulinic and formic acids and the furfural derivatives fragment to produce organic acids. For the second step supercritical water liquefaction stage, the levulinic acid and furfural compounds crack into smaller ketones, hydrocarbons and CO_2. Decarboxylation of levulinic acid produces lighter hydrocarbons in the C_5-C_7 range, while smaller intermediates can form aromatic rings and cyclic hydrocarbons via cyclization and aromatization reactions. The hydrothermal liquefaction of the similarly chemically structured hemicellulose would follow a similar degradation pathway.

The two-step hydrothermal liquefaction mechanism for lignin has also been discussed [96,97]. Under subcritical water conditions the depolymerization of lignin through cleavage of ether linkages (β-O-4 bonds) produces phenolic monomers (guaiacol, catechol, vanillin). Followed by dehydration and condensation of the phenolic compounds into heavier phenolic oligomers, which have the potential to act as char precursors. The supercritical water send step involves cracking of radical species where the phenolic compounds can form alkylphenols, cresols and benzene derivatives. Decarboxylation reactions reduce the oxygen content, forming aromatic compounds and CO_2. Aromatization reactions may results in the formation of PAH or alkylated aromatic compounds.

The proposed reaction mechanism for the two-step hydrothermal liquefaction process shown in Fig. 11 is developed from these previous studies. Based on the reaction timeline under subcritical conditions, the reactions can be divided into three stages, initial stage, intermediate stage and secondary stage. Hydrolysis is generally the initial stage occurring in a low temperature range (below 200 °C) and consists of the partial depolymerization of biomass macromolecules into their monomers [90,98]. Hydrolysis breaks polymeric bonds (glycosidic, ester, peptide) in the presence of water, yielding monomers and oligomers such as sugars, amino acids, and fatty acids [99].

As temperature increases (250–300 °C) the intermediate stage involves enhanced recombination of the reactive fragments and other larger molecules are dissolved into a liquid phase to form a bio-oil [90,100]. In this range of temperature, depolymerization breaks down the large polymeric structures into smaller oligomers or monomers. Under subcritical conditions, hydrolysis and depolymerization might work simultaneously. For example, in cellulose the β-1,4 glycosidic bonds are hydrolysed by water while the crystalline structure of cellulose simultaneously undergoes depolymerization into shorter oligomers leading to cellulose swelling [64,101,102]. When the temperature reaches above 300 °C, the second stage takes place and promotes further reaction such as fragmentation, dehydration to form furfural derivates and organic acid. Dehydration removes water from intermediates to form unsaturated compounds [103]. Monosaccharides from cellulose and hemicellulose hydrolysis are converted into furfural and 5-HMF through dehydration reaction [99,100].

Furfural from pentose: $C_5H_{10}O_5 \rightarrow C_5H_4O_2 + 3H_2O$

5-HMF from hexoses: $C_6H_{12}O_6 \rightarrow C_6H_6O_3 + 3H_2O$

The harsh hydrothermal liquefaction conditions may enhance the possibility of repolymerization that can generate heavy oils or solid char through secondary reactions [103,104]. Repolymerization is a secondary reaction that can occur during hydrothermal liquefaction, particularly when unstable intermediates such as furans, phenolics, and aldehydes condense or polymerize back into larger and more complex molecules. It competes with the desired reactions like decarboxylation and cracking that reduce the bio-oil quality by forming heavier, oxygen-rich components or solid char [26,53].

When water crosses the critical point, the dielectric constant becomes reduced and becomes like a non-polar organic solvent [105,106]. Under this conditions, water dissolves non-polar products, enhancing phase mixing and rapid reactions leading to free-radical reactions and thermal cracking dominate over ionic reactions [64,107–109]. Thermal cracking of intermediates focuses on degradation of carbohydrates, lignin fragments, or fatty acids into smaller hydrocarbons [25,110].

Cracking contributes to bio-oil formation by breaking the long chain oligomers or unstable intermediates into shorter molecules (C_5 - C_{20}), reducing molecular weight and improves volatility to move the mixture closer to the bio-oil range [111,112]. Other than that, decarboxylation, cyclization, and aromatization are also involved in the supercritical step. Decarboxylation become one of the significant reactions in bio-oil formation by reducing the oxygen content to form CO_2 and aromatic compounds combining via aromatization and cyclization to form cyclic hydrocarbons [90,91].

Overall, both one-step and two-step hydrothermal liquefaction under subcritical and supercritical condition can convert lignocellulosic biomass into bio-oil, biochar, aqueous phase and gaseous product. The highest percentage of bio-oil production from one-step hydrothermal liquefaction was 22.7 % at an elevated biomass concentration (1:5 w/w biomass to water ratio), a reaction temperature of 350 °C, and a reaction duration of 60 min. The maximum bio-oil yield for the two-step hydrothermal liquefaction method was 25.44 %, approximately 12 % greater than that of the one-step process, achieved at a biomass to water ratio of 1:10 w/w, a subcritical water reaction temperature of 250 °C for 30 min, and a supercritical water temperature of 400 °C for 60 min.

The two-step hydrothermal liquefaction process demonstrates several advantages over the one-step method for bio-oil quality and content (Fig. 12). Notably, it produces a significantly higher hydrocarbon fraction (3.49 % versus 1.46 %), which enhances the energy density and overall fuel properties of the bio-oil [113,114]. Furthermore, the two-step process yields a considerably lower proportion of phenolic compounds (38.69 % versus 59.21 %), indicating a reduction in oxygenated aromatic species that typically compromise stability and necessitate extensive upgrading. The slightly reduced presence of terpenoids and PAH derivatives in the two-step process product bio-oil also suggests a cleaner product with fewer complex high-molecular-weight components.

Despite the two-step hydrothermal liquefaction process demonstrating a greater concentration of total oxygenates (41.28 % compared to 23.82 %), this disadvantage is mitigated by the enhanced hydrocarbon yield and the decreased presence of phenolic compounds, rendering the product more appropriate for subsequent refining and hydrodeoxygenation [115,116]. Overall, the two-step hydrothermal liquefaction process offers a more hydrocarbon-rich and chemically balanced bio-oil, which aligns better with the requirements for advanced biofuel production.

Conversely, the two-step hydrothermal liquefaction process generates greater quantities of CO_2 and CH_4 than the one-step procedure. The detection of CO_2 and CH_4 in the gaseous product signifies that decarboxylation and reforming reactions transpire to eliminate oxygen from the bio-oil, thereby enhancing its quality. At a biomass-to-water ratio of 1:10 (w/w), the two-step hydrothermal liquefaction produces CO_2 concentrations that are 24.7 times more and CH_4 concentrations that are 2.7 times greater than those from the one-step method. Methane is a significant fuel gas with a high calorific value, serving as an energy source for the hydrothermal liquefaction process. The elevated CO_2 content indicates substantial decarboxylation of biomass, enhancing the quality of bio-oil. Moreover, the two-step hydrothermal liquefaction process decreases the concentration of chemicals in the aqueous phase, facilitating wastewater treatment and decreasing the levels of hydrocarbon by-products.

A further consideration to develop the process would be detailed assessment of the energy efficiency of the two-step process compared to the one-step system, including a mass and energy balance. In addition, a techno-economic assessment would be able to assess the additional energy costs due to extended residence times and higher temperatures versus the added value of the increased bio-oil yield and improved oil composition of the two-step process. Also, if the product bio-oil is to be considered as a potential viable alternative fuel, full characterisation of the fuel properties of the bio-oil would be required. Finally, consideration of scale-up and development of a full process flow and plant design would be required for an industrial/commercial feasibility assessment.

4. Conclusions

The two-step hydrothermal liquefaction strategy, encompassing both subcritical and supercritical phases, offers a substantial advancement over the conventional single-stage process. Notably, the two-step configuration achieves a ~12 % enhancement in bio-oil yield and simultaneously improves oil quality decarboxylation and deoxygenation. The improved quality of the bio-oil is further evidenced by the formation of CO_2 as a product of decarboxylation occurring under supercritical conditions in the second hydrothermal liquefaction stage. Moreover, the preferential formation of C10 – C20 hydrocarbons highlights the role of extended reaction kinetics and phase-specific thermal

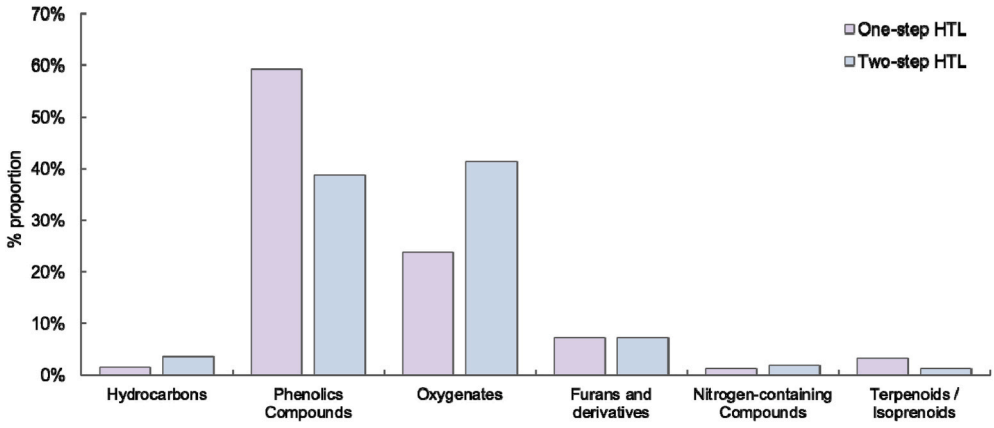

Fig. 12. Bio-oil composition comparison between one-step and two-step hydrothermal liquefaction.

pathways in facilitating the progressive breakdown and reassembly of lignocellulosic matrices into complex, higher molecular-weight hydrocarbon networks. These findings underscore the mechanistic advantage of staged hydrothermal liquefaction of biomass for optimizing both yield and product quality. In this work, improvements in bio-oil quality were evaluated primarily through compositional changes; however, we acknowledge that a full physicochemical characterization (CHNSO, HHV, density, viscosity, moisture) is necessary for direct comparability with other hydrothermal liquefaction studies. Future work will therefore include these analyses to more comprehensively assess the impact of one-step and two-step hydrothermal liquefaction on bio-oil properties and fuel quality.

CRediT authorship contribution statement

Christyfani Sindhuwati: Writing – original draft, Methodology, Investigation. **Mohamad A. Nahil:** Methodology. **Paul T. Williams:** Writing – review & editing, Supervision, Funding acquisition, Conceptualization.

Acknowledgements

This research was funded by the Indonesia Endowment Fund for Education (Lembaga Pengelola Dana Pendidikan – LPDP), Ministry of Finance of the Republic of Indonesia, whose support is gratefully acknowledged.

Data availability

Data will be made available on request.

References

[1] M.E. El-Hefnawy, S. Alhayyani, M.M. El-Sherbiny, A. El-Fatah Abomohra, M. Al-Harbi, Endogenous bioethanol production by solid-state prefermentation for enhanced crude bio-oil recovery through integrated hydrothermal liquefaction of seaweeds, J. Clean. Prod. 355 (2022) 131811, https://doi.org/10.1016/j.jclepro.2022.131811.

[2] R.F. Beims, Y. Hu, H. Shui, C. Xu, Hydrothermal liquefaction of biomass to fuels and value-added chemicals: products applications and challenges to develop large-scale operations, Biomass Bioenergy 135 (2020), https://doi.org/10.1016/j.biombioe.2020.105510.

[3] A.R.K. Gollakota, N. Kishore, S. Gu, A review on hydrothermal liquefaction of biomass, in: Renewable and Sustainable Energy Reviews, vol. 81, Elsevier Ltd, 2018, pp. 1378–1392, https://doi.org/10.1016/j.rser.2017.05.178.

[4] J.A. Ramirez, R.J. Brown, T.J. Rainey, A Review of Hydrothermal Liquefaction Bio-Crude Properties and Prospects for Upgrading to Transportation Fuels, vol. 8, 2015, pp. 6765–6794, https://doi.org/10.3390/en8076765.

[5] X. Hu, M. Gholizadeh, Progress of the applications of bio-oil, Renew. Sustain. Energy Rev. 134 (2020) 110124, https://doi.org/10.1016/J.RSER.2020.110124.

[6] S. Wijeyekoon, K. Torr, H. Corkran, P. Bennett, Commercial Status of Direct Thermochemical Liquefaction Technologies, 2020.

[7] X. Gu, N. Pang, Y. Qiu, X. Fu, Y. Yao, S. Chen, Systematic evaluation of fractionation and valorization of lignocellulose via two-stage hydrothermal liquefaction, Fuel 310 (2022), https://doi.org/10.1016/j.fuel.2021.122358.

[8] S. Leng, H. Jiao, T. Liu, W. Pan, J. Chen, J. Chen, H. Huang, H. Peng, Z. Wu, L. Leng, W. Zhou, Co-liquefaction of Chlorella and soybean straw for production of bio-crude: effects of reusing aqueous phase as the reaction medium. https://doi.org/10.1016/j.scitotenv.2022.153348, 2022.

[9] L. Qian, J. Ni, W. Xu, C. Yuan, S. Wang, Y. Hu, H. Gu, Phycocyanin to biocrude via the integration of isothermal/fast hydrothermal liquefaction and aqueous phase recirculation: reaction products and process analyses. https://doi.org/10.1016/j.fuel.2022.126226, 2022.

[10] J.S. Martinez-Fernandez, S. Chen, Sequential Hydrothermal Liquefaction characterization and nutrient recovery assessment. https://doi.org/10.1016/j.algal.2017.05.022, 2017.

[11] J. Zimmermann, K. Raffelt, N. Dahmen, Sequential hydrothermal processing of sewage sludge to produce low nitrogen biocrude, Processes 9 (3) (2021) 491, https://doi.org/10.3390/PR9030491, 2021, Vol. 9, Page 491.

[12] J. Chen, J. Zhang, W. Pan, G. An, Y. Deng, Y. Li, Y. Hu, Y. Xiao, T. Liu, S. Leng, J. Chen, J. Li, H. Peng, L. Leng, W. Zhou, A novel strategy to simultaneously enhance bio-oil yield and nutrient recovery in sequential hydrothermal liquefaction of high protein microalgae. https://doi.org/10.1016/j.enconman.2022.115330, 2022.

[13] C. Jazrawi, P. Biller, Y. He, A. Montoya, A.B. Ross, T. Maschmeyer, B.S. Haynes, Two-stage hydrothermal liquefaction of a high-protein microalga, Algal Res. 8 (2015) 15–22, https://doi.org/10.1016/j.algal.2014.12.010.

[14] X. Ma, Z. Li, Q. Yang, R. Wu, H. Ben, J. Wu, Microwave-assisted two-stage hydrothermal liquefaction of Spirulina to produce high-quality bio-oil with low-carbon ketones, J. Anal. Appl. Pyrolysis 171 (2023) 105955, https://doi.org/10.1016/J.JAAP.2023.105955.

[15] B. Motavaf, S.H. Capece, T. Eldor, P.E. Savage, Recovery of energy and nitrogen via two-stage valorization of food waste, Cite Ind. Eng. Chem. Res. 2022 (2022), https://doi.org/10.1021/acs.iecr.2c00200.

[16] Y. Tong, T. Yang, B. Li, X. Kai, R. Li, Two-stage liquefaction of sewage sludge in methanol-water mixed solvents with low-medium temperature, J. Supercrit. Fluids 168 (2021) 105094, https://doi.org/10.1016/j.supflu.2020.105094.

[17] K. Wu, X. Zhang, X. Li, Q. Yuan, R. Liu, Investigation of hydrochar properties and bio-oil composition from two-stage hydrothermal treatment of dairy manure, Fuel 339 (2023) 126945, https://doi.org/10.1016/j.fuel.2022.126945.

[18] S. Long, H. Jiang, J. Shi, X. Ai, Z. Que, H. Nie, C.C. Xu, R. Huang, Y. Fu, W. Yang, Separated two-stage hydrothermal liquefaction of livestock manure for high-quality bio-oil with low-nitrogen content: insights on nitrogen migration and evolution, Chem. Eng. J. 477 (2023) 146999, https://doi.org/10.1016/J.CEJ.2023.146999.

[19] C.E. Rostad, W.E. Pereira, Kovats and lee retention indices determined by gas chromatography/mass spectrometry for organic compounds of environmental interest, J. High Resolut. Chromatogr. 9 (6) (1986) 328–334, https://doi.org/10.1002/JHRC.1240090603.

[20] D.L. Vassilaros, R.C. Kong, D.W. Later, M.L. Lee, Linear retention index system for polycyclic aromatic compounds : critical evaluation and additional indices, J. Chromatogr. A 252 (C) (1982) 1–20, https://doi.org/10.1016/S0021-9673(01)88394-1.

[21] J. Akhtar, N.A.S. Amin, A review on process conditions for optimum bio-oil yield in hydrothermal liquefaction of biomass, Renew. Sustain. Energy Rev. 15 (3) (2011) 1615–1624, https://doi.org/10.1016/J.RSER.2010.11.054.

[22] D.P. Vadlamudi, M. Pecchi, H. Sudibyo, J.W. Tester, Direct and two-stage hydrothermal liquefaction of chicken manure: impact of reaction parameters on biocrude oil upgradation, ACS Sustain. Chem. Eng. 12 (10) (2024) 4300–4313, https://doi.org/10.1021/ACSSUSCHEMENG.3C08579/SUPPL_FILE/SC3C08579_SI_001.PDF.

[23] T.H. Saheer, *Hydrothermal Liquefaction of Waste Lignocellulosic Feedstocks from Agricultural, Urban, and Forest Waste Streams for The Production of Biofuels* [Aalborg University]. https://doi.org/10.54337/aau466209855, 2021.

[24] M. Kumar, A. Olajire Oyedun, A. Kumar, A review on the current status of various hydrothermal technologies on biomass feedstock, Renew. Sustain. Energy Rev. 81 (2018) 1742–1770, https://doi.org/10.1016/j.rser.2017.05.270.

[25] A. Mathanker, S. Das, D. Pudasainee, M. Khan, A. Kumar, R. Gupta, A review of hydrothermal liquefaction of biomass for biofuels production with a special focus on the effect of process parameters, Co-Solvents, and extraction solvents. https://doi.org/10.3390/en14164916, 2021.

[26] N. Ghavami, K. Özdenkçi, G. Salierno, M. Björklund-Sänkiaho, C. De Blasio, Analysis of operational issues in hydrothermal liquefaction and supercritical water gasification processes: a review, Biomass Convers. Biorefinery 13 (14) (2023) 12367–12394, https://doi.org/10.1007/S13399-021-02176-4.

[27] M. Wörner, U. Hornung, S. Karagöz, T. Zevaco, N. Dahmen, Focus on hydrochars produced from hydrothermal liquefaction of beech wood, soda lignin and black liquor, Eur. J. Wood Wood Prod. 83 (2) (2025), https://doi.org/10.1007/s00107-025-02214-2.

[28] A. Hussain, A. Kandari, S. Kotiyal, V. Kumar, S. Upadhyay, W. Ahmad, A. Singh, S. Kumar, Hydrothermal liquefaction for biochar production from finger millet waste: its valorisation, process optimization, and characterization, RSC Adv. 14 (34) (2024) 24492–24502, https://doi.org/10.1039/d4ra03945a.

[29] S.K. Das, G.K. Ghosh, R.K. Avasthe, K. Sinha, Compositional heterogeneity of different biochar: effect of pyrolysis temperature and feedstocks, J. Environ. Manag. 278 (2021), https://doi.org/10.1016/j.jenvman.2020.111501.

[30] A.R. Issifu, C. Zhang, Assessing the potential of biomass hydrothermal liquefaction hydrochar for soil amendment: chemical/physical characterization and water holding capacity and retention. https://doi.org/10.3390/w17040504, 2025.

[31] M. Varkolu, S. Gundekari, V. Chandra Sekhar Palla, P. Kumar, S. Bhattacharjee, T. Vinodkumar, Recent advances in biochar production, characterization, and environmental applications. https://doi.org/10.3390/catal15030243, 2025.

[32] R.H. Teoh, A.S. Mahajan, S.R. Moharir, N. Abdul Manaf, S. Shi, S. Thangalazhy-Gopakumar, A review on hydrothermal treatments for solid, liquid and gaseous fuel production from biomass, Energy Nexus 14 (2024) 100301, https://doi.org/10.1016/J.NEXUS.2024.100301.

[33] A.S. Jatoi, A.A. Shah, J. Ahmed, S. Rehman, S.H. Sultan, A.K. Shah, A. Raza, N. M. Mubarak, Z. Hashmi, M.A. Usto, M. Murtaza, Hydrothermal liquefaction of Lignocellulosic and protein-containing biomass: a comprehensive review, Catalysts 12 (12) (2022) 1621, https://doi.org/10.3390/CATAL12121621, 2022, Vol. 12, Page 1621.

[34] J. Chopra, D. Mahesh, A. Yerrayya, R. Vinu, R. Kumar, R. Sen, Performance enhancement of hydrothermal liquefaction for strategic and sustainable valorization of de-oiled yeast biomass into green bio-crude, J. Clean. Prod. 227 (2019) 292–301, https://doi.org/10.1016/J.JCLEPRO.2019.04.147.

[35] M. Thorson, H. Heeres, B. Van de Belt, D. Castello, A. Funke, D. Howe, P. Valdez, Production of Chemicals and Materials from Direct Thermochemical Liquefaction Potential: Applications, Status, Outlook and Challenges, 2024.

[36] J. Watson, Y. Zhang, B. Si, W.T. Chen, R. de Souza, Gasification of biowaste: a critical review and outlooks, Renew. Sustain. Energy Rev. 83 (2018) 1–17, https://doi.org/10.1016/J.RSER.2017.10.003.
[37] G. Yu, Y. Zhang, L. Schideman, T. Funk, Z. Wang, Distributions of carbon and nitrogen in the products from hydrothermal liquefaction of low-lipid microalgae, Energy Environ. Sci. 4 (11) (2011) 4587–4595, https://doi.org/10.1039/C1EE01541A.
[38] S. Ranjbar, F.X. Malcata, Hydrothermal liquefaction: how the holistic approach by Nature will help solve the environmental conundrum. https://doi.org/10.3390/molecules28248127, 2023.
[39] B. Zhang, Q. Lin, Q. Zhang, K. Wu, W. Pu, M. Yang, Y. Wu, Catalytic hydrothermal liquefaction of Euglena sp. microalgae over zeolite catalysts for the production of bio-oil. https://doi.org/10.1039/c6ra28747f, 2017.
[40] T. Wang, D. Zhang, H. Shi, S. Wang, B. Wu, J. Jia, Z. Feng, W. Zhao, Z. Chang, D. Z. Husein, Two birds with one stone: High-Quality utilization of COVID-19 waste masks into Bio-Oil, pyrolytic gas, and eco-friendly biochar with adsorption applications. https://doi.org/10.3390/c10030070, 2024.
[41] B. Zhang, B. Kumar Biswal, J. Zhang, R. Balasubramanian, Hydrothermal treatment of biomass feedstocks for sustainable production of chemicals, fuels, and materials: progress and perspectives. https://doi.org/10.1021/acs.chemrev.2c00673, 2023.
[42] T.M. Brown, P. Duan, P.E. Savage, Hydrothermal Liquefaction and Gasification of Nannochloropsis sp, Energy Fuel. (2010), https://doi.org/10.1021/ef100203u.
[43] J. Watson, T. Wang, B. Si, W.-T. Chen, A. Aierzhati, Y. Zhang, Valorization of hydrothermal liquefaction aqueous phase: pathways towards commercial viability, Prog. Energy Combust. Sci. 77 (2019) 100819, https://doi.org/10.1016/j.pecs.2019.100819.
[44] P.J. Valdez, M.C. Nelson, H.Y. Wang, X.N. Lin, P.E. Savage, Hydrothermal liquefaction of Nannochloropsis sp.: systematic study of process variables and analysis of the product fractions, Biomass Bioenergy 46 (2012) 317–331, https://doi.org/10.1016/j.biombioe.2012.08.009.
[45] B. Bai, Y. Liu, X. Meng, C. Liu, H. Zhang, W. Zhang, H. Jin, Experimental investigation on gasification characteristics of polycarbonate (PC) microplastics in supercritical water, J. Energy Inst. 93 (2) (2020) 624–633, https://doi.org/10.1016/j.joei.2019.06.003.
[46] L.B.S. Thomsen, P.N. Carvalho, J.S. dos Passos, K. Anastasakis, K. Bester, P. Biller, Hydrothermal liquefaction of sewage sludge; energy considerations and fate of micropollutants during pilot scale processing, Water Res. 183 (2020), https://doi.org/10.1016/j.watres.2020.116101.
[47] M. Déniel, G. Haarlemmer, A. Roubaud, E. Weiss-Hortala, J. Fages, Modelling and predictive Study of hydrothermal liquefaction: application to food processing residues, Waste and Biomass Valorization 8 (6) (2017) 2087–2107, https://doi.org/10.1007/S12649-016-9726-7.
[48] J.L. Faeth, P.J. Valdez, P.E. Savage, Fast hydrothermal liquefaction of nannochloropsis sp. to produce biocrude. https://doi.org/10.1021/ef301925d, 2013.
[49] R.B. Madsen, M. Glasius, How do hydrothermal liquefaction conditions and feedstock type influence product distribution and elemental composition? Ind. Eng. Chem. Res. 58 (37) (2019) 17583–17600, https://doi.org/10.1021/acs.iecr.9b02337.
[50] R.B. Madsen, P. Biller, M.M. Jensen, J. Becker, B.B. Iversen, M. Glasius, Predicting the chemical composition of aqueous phase from hydrothermal liquefaction of model compounds and biomasses, Energy Fuels 30 (12) (2016) 10470–10483, https://doi.org/10.1021/ACS.ENERGYFUELS.6B02007.
[51] X. Zhao, Y. Xia, L. Zhan, B. Xie, B. Gao, J. Wang, Hydrothermal treatment of E-Waste plastics for tertiary recycling: product slate and decomposition mechanisms. https://doi.org/10.1021/acssuschemeng.8b05147, 2018.
[52] D. Castello, T.H. Pedersen, L.A. Rosendahl, Continuous hydrothermal liquefaction of biomass: a critical review, Energies 11 (11) (2018) 3165, https://doi.org/10.3390/EN11113165, 2018, Vol. 11, Page 3165.
[53] F. Ahmad, T.R.K.C. Doddapaneni, S.S. Toor, T. Kikas, Reaction mechanism and kinetics of hydrothermal liquefaction at Sub- and supercritical conditions: a review, Biomass 5 (1) (2025) 9, https://doi.org/10.3390/BIOMASS5010009, 2025, Vol. 5, Page 9.
[54] Y. Chen, R. Mu, M. Yang, L. Fang, Y. Wu, K. Wu, Y. Liu, J. Gong, Catalytic hydrothermal liquefaction for bio-oil production over CNTs supported metal catalysts, Chem. Eng. Sci. 161 (2017) 299–307, https://doi.org/10.1016/j.ces.2016.12.010.
[55] C. Ma, J. Geng, D. Zhang, X. Ning, Hydrothermal liquefaction of macroalgae: influence of zeolites based catalyst on products, J. Energy Inst. 93 (2) (2020) 581–590, https://doi.org/10.1016/j.joei.2019.06.007.
[56] P. Duan, P.E. Savage, Catalytic treatment of crude algal bio-oil in supercritical water: optimization studies, Energy Environ. Sci. (2011) 1447–1456, https://doi.org/10.1039/c0ee00343c.
[57] W. Wang, Y. Xu, X. Wang, B. Zhang, W. Tian, J. Zhang, Hydrothermal liquefaction of microalgae over transition metal supported TiO2 catalyst, Bioresour. Technol. 250 (2018) 474–480, https://doi.org/10.1016/j.biortech.2017.11.051.
[58] J. Lu, J. Zhang, Z. Zhu, Y. Zhang, Y. Zhao, R. Li, J. Watson, B. Li, Z. Liu, Simultaneous production of biocrude oil and recovery of nutrients and metals from human faeces via hydrothermal liquefaction, Energy Convers. Manag. 134 (2017) 340–346, https://doi.org/10.1016/J.ENCONMAN.2016.12.052.
[59] Y. Guo, S. Wang, Y. Gong, D. Xu, X. Tang, H. Ma, Partial oxidation of municipal sludge with activited carbon catalyst in supercritical water, J. Hazard Mater. 180 (1–3) (2010) 137–144, https://doi.org/10.1016/j.jhazmat.2010.04.005.
[60] S. Raikova, H. Smith-Baedorf, R. Bransgrove, O. Barlow, F. Santomauro, J. L. Wagner, M.J. Allen, C.G. Bryan, D. Sapsford, C.J. Chuck, Assessing hydrothermal liquefaction for the production of bio-oil and enhanced metal recovery from microalgae cultivated on acid mine drainage, Fuel Process. Technol. 142 (2016) 219–227, https://doi.org/10.1016/J.FUPROC.2015.10.017.
[61] Z. Zhu, L. Rosendahl, S.S. Toor, D. Yu, G. Chen, Hydrothermal liquefaction of barley straw to bio-crude oil: effects of reaction temperature and aqueous phase recirculation, Appl. Energy 137 (2015) 183–192, https://doi.org/10.1016/J.APENERGY.2014.10.005.
[62] G. Ischia, H. Sudibyo, A. Miotello, J.W. Tester, L. Fiori, J.L. Goldfarb, Identifying the transition from hydrothermal carbonization to liquefaction of biomass in a batch System. https://doi.org/10.1021/acssuschemeng.3c07731, 2024.
[63] P.T. Williams, J. Onwudili, Composition of products from the supercritical water gasification of glucose: a model biomass compound, Ind. Eng. Chem. Res. 44 (23) (2005) 8739–8749, https://doi.org/10.1021/IE050733Y.
[64] L.K. Tolonen, Subcritical and supercritical water as a cellulose solvent. http://urn.fi/URN, 2016. ISBN:978-952-60-7025-4.
[65] J. Remón, G. Zapata, L. Oriol, J.L. Pinilla, I. Suelves, A novel 'sea-thermal', synergistic co-valorisation approach for biofuels production from unavoidable food waste (almond hulls) and plastic residues (disposable face masks), Chem. Eng. J. 449 (2022) 137810, https://doi.org/10.1016/J.CEJ.2022.137810.
[66] F. Conti, S.S. Toor, T.H. Pedersen, A.H. Nielsen, L.A. Rosendahl, Biocrude production and nutrients recovery through hydrothermal liquefaction of wastewater irrigated willow, Biomass Bioenergy 118 (2018) 24–31, https://doi.org/10.1016/J.BIOMBIOE.2018.07.012.
[67] N.C. Kokkinos, E. Emmanouilidou, A. Psalidas, Waste to Sustainable Biocrude Production: a Biorefinery Approach, 2025, pp. 167–181, https://doi.org/10.1007/978-3-031-85036-3_7.
[68] Z. Zhu, Z. Liu, Y. Zhang, B. Li, H. Lu, N. Duan, B. Si, R. Shen, J. Lu, Recovery of reducing sugars and volatile fatty acids from cornstalk at different hydrothermal treatment severity, Bioresour. Technol. 199 (2016) 220–227, https://doi.org/10.1016/J.BIORTECH.2015.08.043.
[69] J. Barbier, N. Charon, N. Dupassieux, A. Loppinet-Serani, L. Mahé, J. Ponthus, M. Courtiade, A. Ducrozet, A.A. Quoineaud, F. Cansell, Hydrothermal conversion of lignin compounds. A detailed study of fragmentation and condensation reaction pathways, Biomass Bioenergy 46 (2012) 479–491, https://doi.org/10.1016/J.BIOMBIOE.2012.07.011.
[70] M. Li, B. Si, Y. Zhang, J. Watson, A. Aierzhati, Reduce recalcitrance of cornstalk using post-hydrothermal liquefaction wastewater pretreatment, Bioresour. Technol. 279 (2019) 57–66, https://doi.org/10.1016/J.BIORTECH.2019.01.095.
[71] N. Baccile, G. Laurent, F. Babonneau, F. Fayon, M.M. Titirici, M. Antonietti, Structural characterization of hydrothermal carbon spheres by advanced solid-state MAS 13C NMR investigations, J. Phys. Chem. C 113 (22) (2009) 9644–9654, https://doi.org/10.1021/JP901582X/SUPPL_FILE/JP901582X_SI_001.PDF.
[72] P. Modugno, M.M. Titirici, Influence of reaction conditions on hydrothermal carbonization of fructose, ChemSusChem 14 (23) (2021) 5271–5282, https://doi.org/10.1002/CSSC.202101348.
[73] Y. Qi, B. Song, Y. Qi, The roles of formic acid and levulinic acid on the formation and growth of carbonaceous spheres by hydrothermal carbonization, RSC Adv. 6 (104) (2016) 102428–102435, https://doi.org/10.1039/C6RA21312J.
[74] B. Zhang, J. Chen, Z. He, H. Chen, S. Kandasamy, Hydrothermal liquefaction of fresh lemon-peel: parameter optimisation and product chemistry, Renew. Energy 143 (2019) 512–519, https://doi.org/10.1016/J.RENENE.2019.05.003.
[75] J. Lappalainen, D. Baudouin, U. Hornung, J. Schuler, K. Melin, S. Bjelicbjelic, F. Vogel, J. Konttinen, T. Joronen, Sub-and supercritical water liquefaction of Kraft Lignin and Black liquor derived Lignin, Energies 13 (2020) 1–42, https://doi.org/10.3390/en13133309.
[76] L. Cao, I.K.M. Yu, Y. Liu, X. Ruan, D.C.W. Tsang, A.J. Hunt, Y.S. Ok, H. Song, S. Zhang, Lignin valorization for the production of renewable chemicals: State-of-the-art review and future prospects, Bioresour. Technol. 269 (2018) 465–475, https://doi.org/10.1016/J.BIORTECH.2018.08.065.
[77] G.C. Laredo, J. Reza, E. Meneses Ruiz, Hydrothermal liquefaction processes for plastics recycling: a review, Clean. Chemi. Eng. 5 (2023) 100094, https://doi.org/10.1016/J.CLCE.2023.100094.
[78] A.A. Shah, K. Sharma, T.H. Seehar, S.S. Toor, J. Sandquist, I. Saanum, T. H. Pedersen, Sub-Supercritical hydrothermal liquefaction of lignocellulose and protein-containing biomass, Fuel 5 (1) (2024) 75–89, https://doi.org/10.3390/FUELS5010005, 2024, Vol. 5, Pages 75-89.
[79] T.L.K. Yong, M. Yukihiko, Kinetic analysis of guaiacol conversion in sub- and supercritical water, Ind. Eng. Chem. Res. 52 (26) (2013) 9048–9059, https://doi.org/10.1021/IE4009748/ASSET/IMAGES/LARGE/IE-2013-009748_0009.JPEG.
[80] J. Akhtar, S.K. Kuang, N.A.S. Amin, Liquefaction of empty palm fruit bunch (EPFB) in alkaline hot compressed water, Renew. Energy 35 (6) (2010) 1220–1227, https://doi.org/10.1016/J.RENENE.2009.10.003.
[81] K. Hirayama, R. Maglinao, E. Barbera, S. Kumar, Production of phenolic monomers from lignin in hydrothermal medium: effect of rapid heating and short residence time, J. Supercrit. Fluids 205 (2024) 106123, https://doi.org/10.1016/J.SUPFLU.2023.106123.
[82] N. Zhou, W.P.D.W. Thilakarathna, Q.S. He, H.P.V. Rupasinghe, A review: depolymerization of lignin to generate high-value Bio-Products: opportunities, challenges, and prospects, Front. Energy Res. 9 (2022) 758744, https://doi.org/10.3389/FENRG.2021.758744/XML.
[83] Y.-Y. Zhao, X.-H. Li, S.-B. Wu, M. Li, Temperature impact on the hydrothermal depolymerization of Cunninghamia lanceolata Enzymatic/Mild acidolysis lignin in subcritical water, Bioresources 11 (1) (2016) 21–32.
[84] A. Swetha, S. ShriVigneshwar, K.P. Gopinath, R. Sivaramakrishnan, R. Shanmuganathan, J. Arun, Review on hydrothermal liquefaction aqueous phase as a valuable resource for biofuels, bio-hydrogen and valuable bio-

chemicals recovery, Chemosphere 283 (2021) 131248, https://doi.org/10.1016/J.CHEMOSPHERE.2021.131248.
[85] M. Thorson, H. Heeres, B. Van de Belt, D. Castello, A. Funke, D. Howe, P. Valdez, Production of Chemicals and Materials from Direct Thermochemical Liquefaction, IEA Bioenergy, International Energy Agency, 2024.
[86] J. Feng, Z. Yang, C. yun Hse, Q. Su, K. Wang, J. Jiang, J. Xu, In situ catalytic hydrogenation of model compounds and biomass-derived phenolic compounds for bio-oil upgrading, Renew. Energy 105 (2017) 140–148, https://doi.org/10.1016/j.renene.2016.12.054.
[87] C. Miao, M. Chakraborty, S. Chen, Impact of reaction conditions on the simultaneous production of polysaccharides and bio-oil from heterotrophically grown Chlorella sorokiniana by a unique sequential hydrothermal liquefaction process, Bioresour. Technol. 110 (2012) 617–627, https://doi.org/10.1016/J.BIORTECH.2012.01.047.
[88] Z.Y. Mahssin, M.M. Zainol, N.A. Hassan, H. Yaacob, M.H. Puteh, N.A. Saidina Amin, Hydrothermal liquefaction bioproduct of food waste conversion as an alternative composite of asphalt binder, J. Clean. Prod. 282 (2021) 125422, https://doi.org/10.1016/J.JCLEPRO.2020.125422.
[89] J. S. dos Passos, S. Chiaberge, P. Biller, Combined hydrothermal liquefaction of polyurethane and Lignocellulosic biomass for improved carbon recovery, Energy Fuel. 35 (13) (2021) 10630–10640, https://doi.org/10.1021/acs.energyfuels.1c01520.
[90] I.A. Basar, H. Liu, H. Carrere, E. Trably, C. Eskicioglu, A review on key design and operational parameters to optimize and develop hydrothermal liquefaction of biomass for biorefinery applications, Green Chem. 23 (4) (2021) 1404–1446, https://doi.org/10.1039/D0GC04092D.
[91] B. Li, Y. Liu, T. Yang, B. Feng, X. Kai, S. Wang, R. Li, Aqueous phase reforming of biocrude derived from lignocellulose hydrothermal liquefaction: conditions optimization and mechanism study, Renew. Energy 175 (2021) 98–107, https://doi.org/10.1016/J.RENENE.2021.04.127.
[92] D. Lachos-Perez, P. César Torres-Mayanga, E.R. Abaide, G.L. Zabot, F. De Castilhos, Hydrothermal carbonization and liquefaction: differences, progress, challenges, and opportunities, in: Bioresource Technology, vol. 343, Elsevier Ltd, 2022, https://doi.org/10.1016/j.biortech.2021.126084.
[93] R.K. Mishra, V. kumar, P. Kumar, K. Mohanty, Hydrothermal liquefaction of biomass for bio-crude production: a review on feedstocks, chemical compositions, operating parameters, reaction kinetics, techno-economic study, and life cycle assessment, in: Fuel, 316, Elsevier Ltd, 2022, https://doi.org/10.1016/j.fuel.2022.123377.
[94] A. Dimitriadis, S. Bezergianni, Hydrothermal liquefaction of various biomass and waste feedstocks for biocrude production: a state of the art review, Renew. Sustain. Energy Rev. 68 (2017) 113–125, https://doi.org/10.1016/J.RSER.2016.09.120.
[95] Y.T. Shah, Energy and Fuel Systems Integration, CRC Press, 2015.
[96] S. Kang, X. Li, J. Fan, J. Chang, Hydrothermal conversion of lignin: a review, Renew. Sustain. Energy Rev. 27 (2013) 546–558, https://doi.org/10.1016/J.RSER.2013.07.013.
[97] M.M. Martins, F. Carvalheiro, F. Gírio, An overview of lignin pathways of valorization: from isolation to refining and conversion into value-added products, Biomass Convers. Biorefinery 14 (3) (2024) 3183–3207, https://doi.org/10.1007/s13399-022-02701-z.
[98] X. Zhao, H. Chen, F. Kong, Y. Zhang, S. Wang, S. Liu, L.A. Lucia, P. Fatehi, H. Pang, Fabrication, characteristics and applications of carbon materials with different morphologies and porous structures produced from wood liquefaction: a review, Chem. Eng. J. 364 (2019) 226–243, https://doi.org/10.1016/J.CEJ.2019.01.159.
[99] Y. Fan, U. Hornung, N. Dahmen, Hydrothermal liquefaction of sewage sludge for biofuel application: a review on fundamentals, current challenges and strategies, Biomass Bioenergy 165 (2022) 106570, https://doi.org/10.1016/J.BIOMBIOE.2022.106570.
[100] Y. Fan, U. Hornung, N. Dahmen, A. Kruse, Hydrothermal liquefaction of protein-containing biomass: study of model compounds for Maillard reactions, Biomass Convers. Biorefinery 8 (4) (2018) 909–923, https://doi.org/10.1007/S13399-018-0340-8/METRICS.
[101] M.J. Cocero, Á. Cabeza, N. Abad, T. Adamovic, L. Vaquerizo, C.M. Martínez, M. V. Pazo-Cepeda, Understanding biomass fractionation in subcritical & supercritical water, J. Supercrit. Fluids 133 (2018) 550–565, https://doi.org/10.1016/J.SUPFLU.2017.08.012.
[102] M. Möller, F. Harnisch, U. Schröder, Hydrothermal liquefaction of cellulose in subcritical water—the role of crystallinity on the cellulose reactivity, RSC Adv. 3 (27) (2013) 11035–11044, https://doi.org/10.1039/C3RA41582A.
[103] R. Ghadge, N. Nagwani, N. Saxena, S. Dasgupta, A. Sapre, Design and scale-up challenges in hydrothermal liquefaction process for biocrude production and its upgradation, Energy Convers. Manag. X 14 (2022) 100223, https://doi.org/10.1016/J.ECMX.2022.100223.
[104] D. Liu, Y. Yu, J.I. Hayashi, B. Moghtaderi, H. Wu, Contribution of dehydration and depolymerization reactions during the fast pyrolysis of various salt-loaded celluloses at low temperatures, Fuel 136 (2014) 62–68, https://doi.org/10.1016/J.FUEL.2014.07.025.
[105] B. Ciuffi, M. Loppi, A.M. Rizzo, D. Chiaramonti, L. Rosi, Towards a better understanding of the HTL process of lignin-rich feedstock, Sci. Rep. 11 (1) (2021), https://doi.org/10.1038/s41598-021-94977-w.
[106] S. Masoumi, V.B. Borugadda, A.K. Dalai, Biocrude oil production via hydrothermal liquefaction of algae and upgradation techniques to liquid transportation fuels, in: S. Nanda, D.-V.N. Vo, P.K. Sarangi (Eds.), Biorefinery of Alternative Resources: Targeting Green Fuels and Platform Chemicals, Springer, Singapore, 2020, pp. 249–270, https://doi.org/10.1007/978-981-15-1804-1_11.
[107] S.P. Mezyk, K.A. Rickman, C.M. Hirsch, M.K. Dail, J. Scheeler, T. Foust, Advanced oxidation and reduction process radical generation in the laboratory and on a large Scale: an overview, Monit. Water Qual. Pollut. Assess. Anal. Remed. (2013) 227–248, https://doi.org/10.1016/B978-0-444-59395-5.00009-1.
[108] G. Brunner, Reactions in hydrothermal and supercritical water, Supercrit. Fluid Sci. Technol. 5 (2014) 265–322, https://doi.org/10.1016/B978-0-444-59413-6.00005-4.
[109] Y. Liu, F. Bai, C.C. Zhu, P.Q. Yuan, Z.M. Cheng, W.K. Yuan, Upgrading of residual oil in sub- and supercritical water: an experimental study, Fuel Process. Technol. 106 (2013) 281–288, https://doi.org/10.1016/J.FUPROC.2012.07.032.
[110] R. Ren, X. Han, H. Zhang, H. Lin, J. Zhao, Y. Zheng, H. Wang, High yield bio-oil production by hydrothermal liquefaction of a hydrocarbon-rich microalgae and biocrude upgrading, Carbon Resour. Convers. 1 (2) (2018) 153–159, https://doi.org/10.1016/J.CRCON.2018.07.008.
[111] F. José de Souza, F. Hamad, J. Utzig, G. do Nascimento, A. Carvalho Ribeiro, H. de Bitencourt Rodrigues, H. França Meier, Reduced-Order model for catalytic cracking of bio-oil, Fluids 10 (7) (2025) 179, https://doi.org/10.3390/FLUIDS10070179, 2025, Vol. 10, Page 179.
[112] D.S. Santosa, L. Rohrbach, H. Heeres, R.H. Venderbosch, A. Heeres, H.J. Heeres, Low molecular weight biobased aromatics from pyrolysis liquids using zeolites: yield improvements by using pyrolysis oil fractions, ACS Omega 10 (2) (2025) 1901–1910, https://doi.org/10.1021/ACSOMEGA.4C03831/ASSET/IMAGES/LARGE/AO4C03831_0009.JPEG.
[113] J. Holladay, Z. Abdullah, J. Heyne, Sustainable Aviation Fuel: Review of Technical Pathways Report, 2020.
[114] S. Van Dyk, J. Su, J.D. Mcmillan, J. John,) N. Saddler, "DROP-IN" BIOFUELS: the Key Role that co-processing will Play in its Production, 2019.
[115] A.V. Bridgwater, Review of fast pyrolysis of biomass and product upgrading, Biomass Bioenergy 38 (2012) 68–94, https://doi.org/10.1016/J.BIOMBIOE.2011.01.048.
[116] R. Wijayapala, A.G. Karunanayake, D. Proctor, F. Yu, C.U. Pittman, T.E. Mlsna, Hydrodeoxygenation (HDO) of bio-oil model compounds with synthesis gas using a water–gas shift catalyst with a Mo/Co/K catalyst, Handb. Clim. Change Mitig. Adapt. (2015) 1–34, https://doi.org/10.1007/978-1-4614-6431-0_79-1.